Ore Geology Reviews 101 (2018) 740–764

Contents lists available at ScienceDirect

Ore Geology Reviews

journal homepage: www.elsevier.com/locate/oregeorev

Origin of the high-temperature Olserum-Djupedal REE-phosphate mineralisation, SE Sweden: A unique contact metamorphic-hydrothermal system

Stefan S. Andersson[a,*], Thomas Wagner[b], Erik Jonsson[c,d], Tobias Fusswinkel[a,b], Magnus Leijd[e], Johan T. Berg[f]

[a] Department of Geosciences and Geography, University of Helsinki, P.O. Box 64 (Gustaf Hällströmin katu 2a), FI-00014 Helsinki, Finland
[b] Institute of Applied Mineralogy and Economic Geology, RWTH Aachen University, Wüllnerstrasse 2, D-52062 Aachen, Germany
[c] Department of Mineral Resources, Geological Survey of Sweden, Box 670, SE-75128 Uppsala, Sweden
[d] Department of Earth Sciences, Uppsala University, Villavägen 16, SE-75266 Uppsala, Sweden
[e] Leading Edge Materials Corp, Skolallén 2B, SE-82141 Bollnäs, Sweden
[f] Chromafora AB, Banvaktsvägen 22, SE-17148 Solna, Sweden

ARTICLE INFO

Keywords:
Olserum
Djupedal
REE
Phosphate
Metasomatism
Halogen fugacity

ABSTRACT

The Swedish part of the Fennoscandian Shield hosts a variety of rare earth element (REE) deposits, including magmatic to magmatic-hydrothermal types. This paper focuses on the origin of the Olserum-Djupedal REE-phosphate mineralisation located in the sparsely studied Västervik region, SE Sweden. Here, mineralisation occurs in three main areas, Olserum, Djupedal and Bersummen. Primary hydrothermal REE mineralisation formed at high temperatures (about 600 °C), leading to precipitation of monazite-(Ce), xenotime-(Y), fluorapatite and minor (Y,REE,U,Fe)-(Nb,Ta)-oxides in veins and vein zones dominated by biotite, amphibole, magnetite and quartz. The veins are hosted primarily by metasedimentary rocks present close to, or within, the contact aureole of a local 1.8 Ga ferroan alkali feldspar granite pluton, but also occur within in the chemically most primitive granite in the outermost part of that pluton. In the Djupedal area, REE-mineralised metasedimentary bodies are extensively migmatised, with migmatisation post-dating the main stage of mineralisation. In the Olserum and Bersummen areas, the REE-bearing veins are cross-cut by abundant pegmatitic to granitic dykes. The field relationships demonstrate a protracted magmatic evolution of the granitic pluton and a clear spatial and temporal relationship of the REE mineralisation to the granite.

The major and trace element chemistry of ore-associated biotite and magnetite support genetic links between all mineralised areas. Biotite mineral chemistry data further demonstrate a distinct chemical trend from metasediment-hosted ore-associated biotite distal to the major contact of the granite to the biotite in the granite-hosted veins. This trend is characterised by a systematic decrease in Mg and Na and a coupled increase in Fe and Ti with proximity to the granite-hosted veins. The halogen compositions of ore-associated biotite indicate elevated contents of HCl and HF in the primary REE mineralising fluid. Calculated $\log(f_{HF}/f_{HCl})$ values in the Olserum area suggest a constant ratio of about −1 at temperatures of 650–550 °C during the evolution of the primary hydrothermal system. In the Djupedal and Bersummen areas, the fluid locally equilibrated at lower $\log(f_{HF}/f_{HCl})$ values down to −2. High Na contents in ore-associated biotite and amphibole, and the abundance of primary ore-associated biotite indicate a K- and Na-rich character of the primary REE mineralising fluid and suggest initial high-temperature K-Na metasomatism. With subsequent cooling of the system, the fluid evolved locally to more Ca-rich compositions as indicated by the presence of the Ca-rich minerals allanite-(Ce) and uvitic tourmaline and by the significant calcic alteration of monazite-(Ce). The later Ca-rich stages were probably coeval with low to medium-high temperature (200–500 °C) Na-Ca metasomatism variably affecting the granite and the wall rocks, producing distinct white quartz-plagioclase rocks.

All observations and data lead us to discard the prevailing model that the REE mineralisation in the Olserum-Djupedal district represents assimilated and remobilised former heavy mineral-rich beds. Instead, we propose that the primary REE mineralisation formed by granite-derived fluids enriched in REE and P that were expelled early during the evolution of a local granitic pluton. The REE mineralisation developed primarily in the contact aureole of this granite and represents the product of a high temperature contact metamorphic-hydrothermal

* Corresponding author.
E-mail address: stefan.andersson@helsinki.fi (S.S. Andersson).

https://doi.org/10.1016/j.oregeorev.2018.08.018
Received 24 February 2018; Received in revised form 9 August 2018; Accepted 14 August 2018
Available online 16 August 2018

mineralising system. The REE mineralisation probably formed synchronously with K-Na and subsequent Na-Ca metasomatism affecting the granite and the wall rocks. The later Na-Ca metasomatic stage is probably related to a regional Na ± Ca metasomatic and associated U ± REE mineralising system operating concurrently with granitic magmatism at c. 1.8 Ga in the Västervik region. This highlights the potential for discovering hitherto unknown REE deposits and for the reappraisal of already known deposits in this part of the Fennoscandian Shield.

1. Introduction

The emplacement of granitic plutons into the Earth's continental crust causes a significant heat input to the immediate wall rocks, inducing contact metamorphism and circulation of hot fluids. The fluids associated with such an environment can be magmatic fluids released from the crystallising pluton, pore fluids in wall rocks, metamorphic fluids produced by devolatilisation in the adjacent wall rocks, and ultimately meteoric water that is convected into hydrothermal systems during later cooling of the pluton (Hansen, 1995; Kesler, 2005; Ingebritsen and Appold, 2012). If these fluids transport significant concentrations of metals, either by extracting them from the magma via an exsolving fluid phase, or due to interaction with the surrounding wall rocks, and if the fluids can be focused into distinct structural pathways or zones, they may form primary magmatic-hydrothermal deposits such as for example porphyry Cu deposits, as well as related metasomatic skarn deposits (Hedenquist and Lowenstern, 1994; Cox, 2005; Heinrich and Candela, 2013). Metasomatism in contact-metamorphic environments occurs almost invariably to some extent, and varies extensively in style, degree and distribution, depending on factors such as chemistry and depth of the granitic pluton (e.g., Barton et al., 1991). Metasomatism is in most cases essential to attain ore-grade concentrations, as aptly shown by rare earth element (REE) deposits associated with fenitisation of the wall rocks during the emplacement of carbonatitic or silica-undersaturated intrusions (e.g., Kresten and Morogan, 1986; Morogan and Woolley, 1988; Morogan, 1989; Sjöqvist et al., 2017; Elliott et al., 2018).

Only a few hydrothermal REE mineralisations associated with granitic plutons are known, including the REE-Th deposit at Las Chacras, Argentina (Lira and Ripley, 1990) and the Kutessay II deposit, Kyrgyzstan (Djenchuraeva et al., 2008). Instead, REE mineralisations are typically associated with other types of intrusions, mainly silica-undersaturated and peralkaline rocks, carbonatites, and their fenitised halos (e.g., Chakhmouradian and Zaitsev, 2012 and references therein). In this perspective, it is essential to study how the REE behave in hydrothermal REE mineralising systems that show a clear spatial relation to granitic (sensu lato) plutons and their associated metasomatic or contact aureoles.

Sweden hosts many REE mineralisations of various deposit types. Of these, the Bastnäs-type skarn deposits (Holtstam and Andersson, 2007; Holtstam et al., 2014; Jonsson et al., 2014) and NYF-type granitic pegmatites like Ytterby (e.g., Nordenskjöld, 1910; Smeds, 1990) have historically been the most important ones. In addition to these, REE are hosted by e.g., apatite-iron oxide deposits such as Kiirunavaara and Malmberget in the Norrbotten region (Frietsch and Perdahl, 1995) and in the Grängesberg-Blötberget deposits in Bergslagen (Jonsson et al., 2016, and references therein), in carbonatites such as the Alnö complex (Morogan and Woolley, 1988; Morogan, 1989), and in peralkaline rocks as in Norra Kärr (e.g., Sjöqvist et al., 2013; Sjöqvist et al., 2017, and references therein). The Palaeoproterozoic, metasedimentary Västervik Formation in south-eastern Sweden is also known to host occurrences of U and variable amounts of REE (e.g., Uytenbogaardt, 1960; Welin, 1966a,b; Hoeve, 1974). These occurrences are mainly associated with various iron oxide mineralisations (Geijer and Magnusson, 1944; Uytenbogaardt, 1960). Yet, modern mineralogical and geochemical studies addressing the origin of these and the associated REE ± U mineralisations are lacking. Understanding the magmatic and hydrothermal processes leading to these different types of mineralisations are important, not least because they may have operated on a regional scale and may potentially provide a link between different mineralisation styles.

This contribution focuses on the Olserum-Djupedal REE mineralisation, which is one of the known but poorly studied types of REE ± U occurrences in the Västervik Formation. This mineralisation includes one of only a few known and well-defined REE deposits (Olserum) in Europe with a NI43-101 certified resource estimate (Reed, 2013; Goodenough et al., 2016). The mineralisation comprises an unusual primary assemblage with abundant monazite-(Ce), xenotime-(Y) and fluorapatite in veins dominated by biotite, amphibole, quartz and magnetite. By expanding on the mineralogical, textural and mineral-chemical framework developed earlier for the REE-bearing minerals (Andersson et al., 2018), this study combines field and petrographic relationships with major element chemistry of the main gangue minerals and with trace element chemistry of biotite and magnetite. This was done in order to understand the relative timing and origin of the mineralisation and to develop an initial mineralisation model. The clear temporal and spatial association of the REE mineralisation with a local granite pluton emplaced at 1.8 Ga, and the strong chemical gradients shown by biotite, and partly by magnetite, in proximity to this granite, lead us to propose a high-temperature contact metamorphic-hydrothermal origin for the Olserum-Djupedal REE mineralisation. This mineralisation and other similar, smaller REE occurrences likely formed as part of a regional-scale metasomatic and REE ± U mineralising event.

2. Geological background

2.1. Regional geology

The Olserum-Djupedal REE mineralisation is situated about 8 km NW of Gamleby in SE Sweden, in the Västervik region (Fig. 1). The discrete mineralisations are all located along the border between the Västervik metasedimentary Formation and the Transscandinavian Igneous Belt (TIB), south of the Svecofennian domain of the Fennoscandian Shield (Gavelin, 1984; Gaál and Gorbatschev, 1987; Gorbatschev, 2004). The Svecofennian domain formed in an accretionary-type orogeny at 1.92–1.77 Ga (e.g., Korja et al., 2006). Its western and southern part is surrounded by the large, NNW-SSE trending TIB complex of plutonic to volcanic units, established along an active continental margin at 1.85–1.65 Ga (Gorbatschev, 2004). The boundary between the Svecofennian domain and the Västervik Formation is broadly defined by the Loftahammar-Linköping Deformation Zone (LLDZ; Fig. 1), comprising several major crustal-scale shear zones active at around 1.8 Ga (Beunk and Page, 2001).

The Västervik Formation is a Palaeoproterozoic metasupracrustal unit that primarily comprises quartzites and meta-arenites, and subordinate meta-argillites and metavolcanic rocks (Gavelin, 1984). Based on the age of the youngest detrital zircons and the age of the intruding Loftahammar-type granitoids (1859 ± 9 Ma; Bergström et al., 2002), Sultan et al. (2005) inferred a depositional age of about 1.88–1.85 Ga for the Västervik sediments. The Loftahammar-type granitoids have traditionally been referred to as the older of two generations of granitoids that intrude the Västervik Formation (e.g., Gavelin, 1984; Kresten, 1986). These older (c. 1.85 Ga) granitoids are usually deformed and

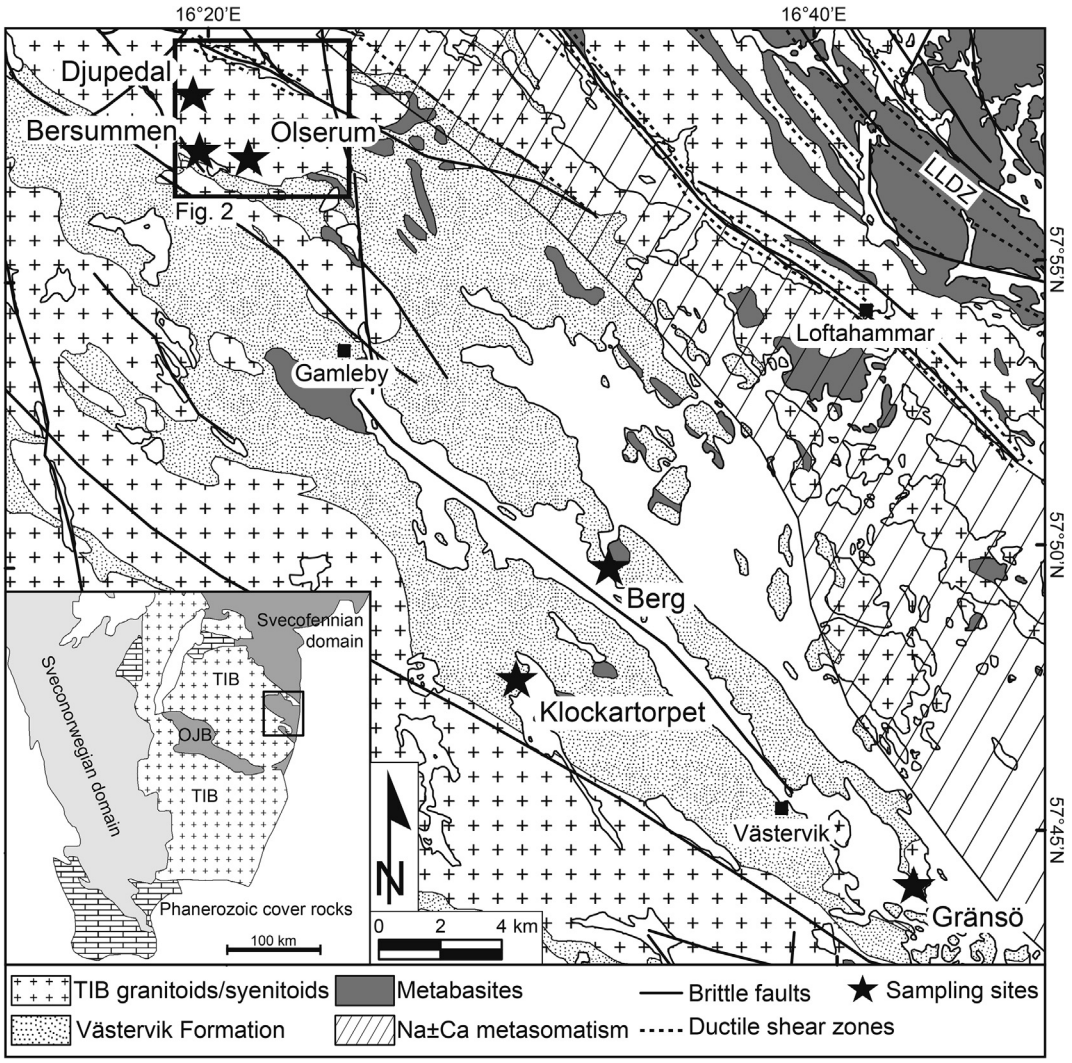

Fig. 1. Geological map of the Västervik region, showing major rock units, structures and sample locations. Modified after Gavelin (1984) and mapping data from the database of the Geological Survey of Sweden (http://www.sgu.se). The location of the detailed geological map of the Olserum-Djupedal district (Fig. 2) is indicated by a black frame. The indicated area of Na ± Ca metasomatism is redrawn from Hoeve (1974). The inset map shows the large-scale geology of southern Sweden, redrawn from Andersen et al. (2009). The white areas without graphical pattern are water. LLDZ: Loftahammar-Linköping Deformation Zone (Beunk and Page, 2001); TIB: Transscandinavian Igneous Belt (Gorbatschev, 2004); OJB: Oskarshamn-Jönköping Belt (Mansfeld et al., 2005).

exhibit an augen gneiss fabric. The younger, mostly structurally isotropic granites belong to the c. 1.81–1.77 Ga suite of TIB-1 granitoids (e.g., Wikström and Andersson, 2004, and references therein; Kleinhanns et al., 2015). In a recent attempt to better understand the tectonic evolution of the long-lived active continental margin magmatism in this part of the Fennoscandian shield, Nolte et al. (2011) and Kleinhanns et al. (2015) proposed a new three-stage tectono-magmatic model, based on petrographical and geochemical re-classification of the granitoids, combined with new zircon U-Pb geochronology. According to this, the first stage (Askersund or TIB-0) stage is characterised by alkali-calcic to calc-alkalic and metaluminous to peraluminous granitoids with a ferroan affinity (cf. Frost et al., 2001), emplaced within an extensional or transtensional regime, at around 1.85 Ga. Subsequently, a compressional regime prevailed at around 1.85–1.81 Ga, followed by intrusion of the TIB-1 magmas, which formed metaluminous Cordilleran-type granitoids; they comprise most of the plutonic rocks in the Västervik region. The final stage is represented by the generation of moderately shallow and local, mostly peraluminous anatectic granites with a ferroan affinity, which formed in an extensional or transtensional regime at or slightly after 1.8 Ga. The metasedimentary rocks of the Västervik Formation were the source for these younger granites, and they mostly show short melt-transport distances. A moderately shallow (at c. 15 km depth) crustal anatectic origin for some of the younger granites in the Västervik region was already suggested by Westra et al. (1969). The formation of these anatectic granites likely coincided with high-temperature/low-pressure metamorphism and related migmatisation (e.g., Kresten, 1971; Kleinhanns et al., 2012). The metamorphic conditions in the Västervik region reached upper amphibolite facies conditions (about 650 °C to 700 °C and < 400 MPa), based on the presence of sillimanite + andalusite + cordierite ± K-feldspar in the Västervik metasediments (Russel, 1969; Elbers, 1971; Kresten, 1971; Gavelin, 1984). The main structural elements in the Västervik Formation are a series of NW-SE trending synclines and anticlines, which locally follow the outlines of the older granitoid massifs (Gavelin, 1984), and are presumably pre- to syn-kinematic with the generation and intrusion of the youngest granites and associated high-grade metamorphism (Westra et al., 1969; Elbers, 1971).

2.2. U ± REE mineralisations in the Västervik region

2.2.1. Historical overview

Prior to extensive, state-funded uranium exploration in Sweden in

the 1950s, the Västervik region was known to host various types of Fe ± Cu ± Mo ± Co mineralisations, which were mined in the 15th century and onwards (Tegengren, 1924; Uytenbogaardt, 1960; Sundblad, 2003, and references therein; Billström et al., 2004). During the uranium exploration period, several occurrences were discovered or reinvestigated for their U potential, including the Olserum-Djupedal district, Gränsö in the Västervik archipelago and Klockartorpet in the central part of the Västervik Formation (Uytenbogaardt, 1960; Welin, 1966a,b; Löfvendahl and Åkerblom, 1976). The REE potential, particularly that of the mineralisation in the Olserum-Djupedal district, was not recognised until the beginning of the 1990s during regional field campaigns targeting REE by the Geological Survey of Sweden, when high contents of these metals were confirmed (Gustafsson, 1992). Interestingly, minor amounts of apatite and "zircon" were found within these ores already in the 1960s (Welin 1966a); potentially misidentifying the abundant xenotime-(Y) as "zircon".

2.2.2. U ± REE mineralisations: types and proposed origin

Uytenbogaardt (1960) recognised three types of U ± REE mineralisation in the Västervik region: 1) quartzite-hosted palaeoplacer deposits containing uraninite and pyrobitumen with fine-grained uraninite inclusions (so-called thucholite); 2) magnetite ore with associated U ± REE minerals; and 3) pegmatites and aplites hosting U ± REE minerals. He also proposed a magmatic origin related to the generation and emplacement of the younger suite of granites for all these U ± REE occurrences. Welin (1966a,b) proposed that the U ± REE mineralisations, including those of the Olserum-Djupedal district and Gränsö, represent heavy mineral-rich palaeobeds (palaeoplacers), which had been extensively remobilised by the anatectic granite, and later enriched and incorporated into associated aplites and pegmatites. In contrast, Hoeve (1974, 1978) postulated a hydrothermal origin for the U ± REE mineralisations and linked them to distinct quartz-plagioclase rocks that formed during Na ± Ca metasomatism along the contact between the Västervik Formation and the older Loftahammar-type granitoids in the north (Fig. 1). Furthermore, he inferred that these metasomatic rocks formed from fluid-driven replacement of metasedimentary rocks of the Västervik Formation and the older granitoids during prograde to peak metamorphism. The U ± REE mineralisations represented the end-product of the metasomatism and were considered younger. Moreover, the emplacement of the younger suite of granites, which in this case most likely corresponds to the anatectic granites, was interpreted to be younger than both the metasomatic rocks and the U ± REE mineralisations. Hoeve (1974), however, also considered the metasomatism and the generation of the younger granites as synchronous processes at different crustal levels during peak metamorphism.

2.2.3. REE mineralisation in the Olserum-Djupedal district

The REE mineralisation in the Olserum-Djupedal district was considered a potential REE prospect following the regional exploration campaign for REE in the beginning of the 1990s (Gustafsson, 1992). Targeted exploration (including surface mapping and core drilling) was conducted by IGE Nordic AB from 2003 to 2008. Tasman Metals Ltd. (now Leading Edge Materials) conducted further exploration, including additional field mapping and core drilling, specifically targeting the REE.

The Olserum-Djupedal district consists of three exposed areas with more extensive REE mineralisation, namely Olserum, Djupedal and Bersummen (Fig. 2), which together comprise the Olserum-Djupedal REE mineralisation. The exploration has so far yielded a NI-43-101 compliant indicated resource estimate of 4.5 Mt at 0.6% total rare earth oxides (TREO) with 33.9% heavy rare earth oxides (HREO) for part of the Olserum area only, which is thus the only defined REE resource in the district (Reed, 2013). The resource in Olserum covers an area of around 400 by 100–150 m and has been drilled to a depth of around 250 m. It consists of six mineralised zones with a NW to SE strike, which are dipping steeply to the NE. The outlined resource represents only a small part of the known mineralised area in the district, and the drilled part of the mineralisation is open at depth.

Previous work focused on characterising the main REE minerals and obtaining preliminary mineral chemistry data of the main phases (Fullerton, 2014). However, this work only covered a limited part of the known mineralisation and exclusively focused on new drill core material from Olserum. Andersson et al. (2018) reported the results of a detailed characterisation of the mineralogy and textural evolution of the REE minerals, combined with major and trace element analyses of all REE phases. They recognised four paragenetic stages of REE mineral formation for the Olserum-Djupedal REE mineralisation, as summarised in Table 1. Furthermore, the paragenetic sequence was interpreted to record an initial high-temperature hydrothermal stage (about 600 °C), which was followed by fluid-mediated dissolution-reprecipitation processes that operated during progressively decreasing temperatures. In addition, it was concluded that local differences in fluid chemistry, especially the Ca content, between the Olserum and Djupedal areas, were important factors in controlling the stabilities of primary REE-bearing ore minerals.

2.2.4. Geology of other sampled locations within the Västervik region

To put the REE mineralisation in the Olserum-Djupedal district into a broader regional context, additional sampling of three other localities in the Västervik region was carried out, at Klockartorpet, Gränsö and Berg (Fig. 1).

Klockartorpet (N 57° 48.0′, E 16° 30.0′) is a palaeoplacer mineralisation in the central part of the Västervik Formation. The palaeoplacer consists of a series of dark layers in quartzite, which contain biotite, muscovite, magnetite, ilmenite, rutile, zircon and minor monazite and U-bearing phases.

Gränsö (N 57° 44′, E 16° 42.5′) is an island in the Västervik archipelago and the outcrops studied are situated on the SW side, around one of the old, now water-filled open pit magnetite mines. The area exposes folded and fine-grained metasedimentary gneisses rich in feldspar (K-feldspar typically), intercalated with coarse-grained F-rich biotite and magnetite bands with variable thicknesses. The bands are occasionally boudinaged and the magnetite displays a granoblastic recrystallised texture. Thin section petrography and energy-dispersive spectroscopy (EDS) demonstrate that magnetite is associated with locally abundant monazite-(Ce) and zircon, and subordinate ilmenite, rutile, xenotime-(Y), fluorapatite, fluorite, uraninite, REE-fluorocarbonates, Sr-bearing barite and Ba-bearing strontianite.

The locality at Berg (N 57° 50.0′, E 16° 33.0′) exposes quartzites and minor intercalated metapelitic layers of the Västervik Formation in several road cuts. These metasedimentary rocks are transected by K-feldspar-dominated migmatitic melt veins (leucosomes), and tourmaline-bearing pegmatitic segregations formed in situ. The migmatitic melt veins contain euhedral magnetite, and the surrounding quartzite is tourmalinised.

3. Material and analytical methods

3.1. Field work and sampling

Four drill cores drilled by Tasman Metals Ltd. in 2012 were logged and sampled in detail at the national Swedish drill core archive of the Geological Survey of Sweden in Malå. Sampling and field mapping in the Olserum-Djupedal district were performed during two consecutive field campaigns in 2015 and 2016. Sampling was aimed at obtaining a representative set of samples of the ore-bearing assemblages from different areas (Olserum, Bersummen and Djupedal; Fig. 2), and samples from the different host rocks in the district (Table 2). Field mapping focused on the geological framework of the district and the relative timing of mineralisation. The samples from the Olserum-Djupedal mineralisation were complemented by samples from other occurrences in the Västervik region (Klockartorpet, Gränsö and Berg; Fig. 1). This

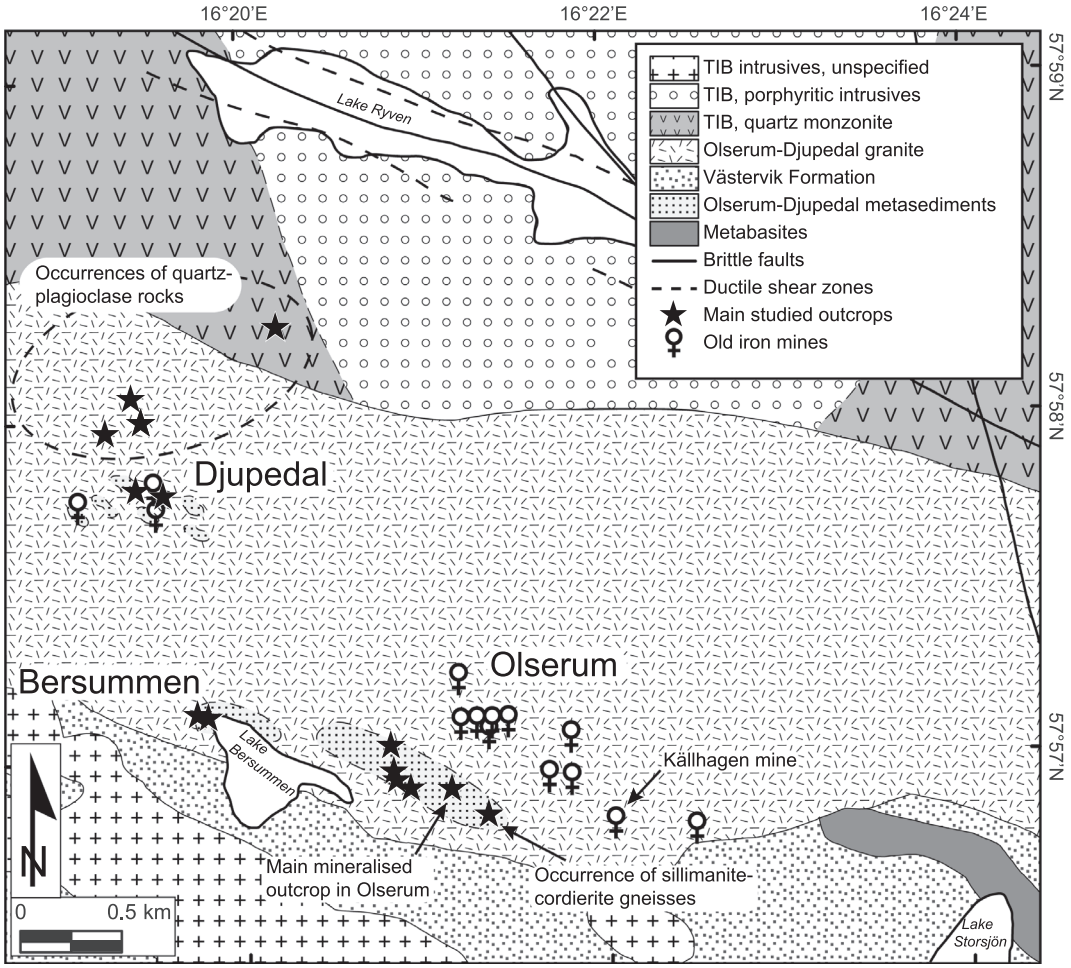

Fig. 2. A simplified geological map of the Olserum-Djupedal district illustrating the locations of the main studied outcrops and old iron mines. Based on new field mapping data of this study and data from the Geological Survey of Sweden (http://www.sgu.se).

sampling was targeted on material containing biotite and magnetite for mineral chemistry analysis.

3.2. Electron-probe microanalysis (EPMA)

Major element analysis was performed on biotite, magnetite, amphibole, tourmaline and minor muscovite and chlorite (all mineral chemical data are available in the online data repository). The analyses were done by wavelength-dispersive electron probe microanalyser (EPMA) using a JEOL JXA-8600 Superprobe at the University of Helsinki, upgraded with SAMx hardware and the XMAs/IDFix/Diss5 analytical and imaging software package. The accelerating voltage used was 15 kV and the beam current 15 nA. All analyses were conducted with a focused beam. A complete list of analytical conditions (radiations, standards, counting times, analyser crystals) used for EPMA analyses is available in the online data repository. Biotite formulae were calculated based on 22 oxygens per formula unit, using K concentrations from LA-ICP-MS because we observed a slight overestimation of K concentrations by EPMA in some biotite analyses. The H_2O content was calculated assuming full occupancy of the OH sites, i.e. (OH + F + Cl) = 4 atoms per formula unit (apfu). All Fe was assumed to be Fe^{2+}. Amphibole formulae were calculated based on

Table 1
Summary of the paragenetic sequence of REE minerals in the Olserum-Djupedal district. See also Fig. 4 in Andersson et al. (2018).

Stage	REE-bearing minerals formed	Key textural observations	Metasomatism (this study)	Temperature
Stage A	Primary xenotime-(Y), monazite-(Ce), fluorapatite, subordinate (Y,REE,U,Fe)-(Nb,Ta)-oxides	(1) Fractured REE minerals	K-Na metasomatism	about 600 °C
Stage B	Xenotime-(Y), monazite-(Ce), allanite-(Ce)	(1) Dissolution-reprecipitation of fluorapatite forming secondary REE-phosphates in fluorapatite, subsequent leaching and remobilisation of REE forming monazite-(Ce) and xenotime-(Y) in fractures and in the surrounding mineral groundmass of fluorapatite; (2) Formation of allanite-(Ce) in fractured primary xenotime-(Y); (3) Replacement of xenotime-(Y) by minor monazite-(Ce)	K-Na metasomatism to Na-Ca metasomatism	400–600 °C
Stage C	Fluorapatite, allanite-(Ce) – ferriallanite-(Ce), xenotime-(Y), monazite-(Ce), uraninite, thorite, columbite-(Fe)	(1) Pervasive to partial alteration of monazite-(Ce); (2) Th-U dissolution-reprecipitation in xenotime-(Y) and monazite-(Ce); (3) Alteration of primary (Y,REE,U;Fe)-(Nb,Ta)-oxides	Na-Ca metasomatism	< 400 °C
Stage D	Bastnäsite-(Ce), synchysite-(Ce)	(1) Alteration and chloritisation of allanite-(Ce) or ferriallanite-(Ce)	Na-Ca metasomatism	< 300 °C

Table 2
Summary of the different ore and rock types mentioned in the text.

Type	Description	Mineralogy	Samples used in this study
Olserum area REE mineralisation	Dominantly biotite-rich veins and vein zones in metasedimentary rocks	Biotite, quartz, amphibole (gedrite), xenotime-(Y), monazite-(Ce), fluorapatite, magnetite, ilmenite, (REE,Y,Th,Ca)-(Nb,Ta)-oxides, cordierite, chlorite, muscovite, andalusite, plagioclase, pyrite, chalcopyrite, galena, zircon, Al-spinel lamellae in magnetite, uraninite, columbite, unidentified Th-U silicates, fluorite, chlorite, rutile, hematite, calcite	OLR12001-78.8, OLR12003-129.7, OLR12003-156.6, OLR12003-172.8, OLR12003-184.7, OLR12003-192.4
Djupedal area REE mineralisation	Biotite dominated ore within large sedimentary bodies in granite	Biotite, xenotime-(Y), monazite-(Ce), magnetite, quartz, fluorapatite, cordierite, allanite-(Ce) - ferriallanite-(Ce), ilmenite, muscovite, amphibole (gedrite, anthophyllite), tourmaline (uvite and schorl-dravite), uraninite, thorite, clinozoisite, staurolite, andalusite, scheelite, ferberite, fluorite, Al-spinel lamellae in magnetite, bastnäsite-(Ce), pyrite, chalcopyrite, chlorite, hematite, rutile, titanite	DJU06, DJU21-2, DJU26
Bersummen area REE mineralisation	Biotite-fluorapatite veins in metasedimentary rocks	Biotite, fluorapatite, amphibole (gedrite), quartz, monazite-(Ce), xenotime-(Y), chlorite, magnetite, staurolite, pyrite, chalcopyrite, unspecified U-mineral, andalusite	BER01
Granite-hosted REE-bearing veins	Biotite-rich veins within granite, surrounded by a thin alteration selvage	Biotite, quartz, magnetite, fluorapatite, monazite-(Ce), xenotime-(Y), ilmenite, muscovite, chlorite, uraninite, hematite, rutile	OLR12003-117.4
Biotite-magnetite schlieren	Hosted in granite	Biotite, magnetite, quartz, allanite-(Ce), monazite-(Ce), xenotime-(Y), ilmenite, Nb-rutile, fluorite, bastnäsite-(Ce), synchysite-(Ce), fluorapatite, uraninite, zircon, pyrite, galena, chlorite, rutile, hematite	KJA01, OLR07
Magnetite-quartz schlieren	Hosted in granite (Fig. 8)	Quartz, magnetite, monazite-(Ce), xenotime-(Y), chloritised biotite	OLR01, BODA01
Olserum-Djupedal granite	Alkali-feldspar granite	K-feldspar, biotite, quartz, plagioclase, muscovite, magnetite, tourmaline (schorl-dravite), zircon, monazite-(Ce), xenotime-(Y), fluorite, fluorapatite, chlorite, hematite	OLR12001-10.6, OLR12003-117.4, OLR12003-117.5, OLR12003-34.3
Olserum metasedimentary host rock	Grey to reddish host rock	Biotite, quartz, plagioclase, muscovite, cordierite, monazite-(Ce), xenotime-(Y)	OLR12004-94.0
Olserum transition zone gneiss	Heterogeneous, unclear protolith	Biotite, K-feldspar, quartz, muscovite, xenotime-(Y), zircon, magnetite	OLR12001-40.9
Djupedal migmatitic gneiss	Migmatitic gneiss, stromatitic	K-feldspar, biotite, quartz, plagioclase, rutile, muscovite, xenotime-(Y), monazite-(Ce), zircon	DJU23
Olserum alteration in granitic gneiss	Alteration zone in Olserum (Fig. 6H)	Biotite, quartz, xenotime-(Y), monazite-(Ce), zircon, plagioclase, ilmenite, pyrite, chalcopyrite, thorite (or other Th-silicates), chlorite, hematite, barite	OLR12
Alteration selvages within granite	Thin alteration selvage around granite-hosted veins	Green to brown biotite, K-feldspar, plagioclase, quartz, magnetite, ilmenite, muscovite, monazite-(Ce), xenotime-(Y), fluorapatite, chlorite, uraninite, hematite, rutile	OLR12003-117.4
Klockartorpet palaeoplacer	Thin black layers in quartzite	Biotite, quartz, magnetite, ilmenite, rutile, zircon, muscovite, monazite, unidentified U-mineral	KLO01
Berg quartzite	Quartz-biotite-plagioclase metasedimentary rock	Quartz, biotite, plagioclase, muscovite, magnetite, ilmenite, zircon, tourmaline (schorl)	BERG02
Berg migmatite	Formed in situ	K-feldspar, quartz, biotite, tourmaline (schorl), magnetite, muscovite, zircon, monazite-(Ce), chlorite, hematite	BERG05
Gränsö magnetite ore	Magnetite-biotite rich layers in metasedimentary rocks	Biotite, magnetite, zircon, monazite-(Ce), quartz, fluorite, ilmenite, uraninite, xenotime-(Y), fluorapatite, REE-fluorocarbonates, barite, strontianite, rutile	GRA01

Table 3
Instrumental parameters used for LA-ICP-MS analysis.

General parameters	
Laser system	Coherent GeoLas Pro MV excimer
Wavelength	193 nm
ICP system	Agilent 7900s ICP mass spectrometer
Plasma gas flow (Ar)	15 L/min
Auxiliary gas flow (He)	0.85 L/min
Carrier gas flow (He)	1 L/min
Magnetite	
Energy density	4 J/cm^2
Repetition rate	5 Hz
Number of laser pulses	250 equal to 50 s of sample ablation
Spot sizes	32, 44, 60 or 90 µm
Isotopes measured	^{24}Mg, ^{27}Al, ^{29}Si, ^{31}P, ^{45}Sc, ^{47}Ti, ^{51}V, ^{52}Cr, ^{55}Mn, ^{56}Fe, ^{57}Fe, ^{59}Co, ^{61}Ni, ^{63}Cu, ^{66}Zn, ^{69}Ga, ^{71}Ga, ^{75}As, ^{88}Sr, ^{89}Y, ^{93}Nb, ^{118}Sn, ^{121}Sb, ^{137}Ba, ^{140}Ce, ^{181}Ta, ^{182}W, ^{208}Pb, ^{232}Th, and ^{238}U
Internal standard	^{57}Fe (EPMA)
External standards	NIST SRM 610, USGS reference glass GSE-1G
Dwell times	0.01 s; U, Th, and W: 0.02 s
Biotite	
Energy density	4 J/cm^2
Repetition rate	10 Hz
Number of laser pulses	500 equal to 50 s of sample ablation
Spot sizes	32, 44 or 60 µm
Isotopes measured	^{7}Li, ^{23}Na, ^{24}Mg, ^{27}Al, ^{29}Si, ^{35}Cl, ^{39}K, ^{42}Ca, ^{45}Sc, ^{49}Ti, ^{51}V, ^{53}Cr, ^{55}Mn, ^{57}Fe, ^{59}Co, ^{60}Ni, ^{66}Zn, ^{71}Ga, ^{85}Rb, ^{88}Sr, ^{89}Y, ^{93}Nb, ^{95}Mo, ^{118}Sn, ^{133}Cs, ^{138}Ba, ^{181}Ta, ^{182}W, ^{205}Tl, and ^{208}Pb
Internal standard	^{27}Al (EPMA)
External standards	NIST SRM 610, USGS reference glass GSE-1G, Sca17
Dwell times	0.01 s; Y and Ca: 0.005 s

(O + OH + F + Cl) = 24 apfu, and H_2O was calculated assuming (OH + Cl + F) = 2 apfu. Ferric iron was calculated based on electroneutrality, using the calculation scheme by Locock (2014), which follows the IMA 2012 amphibole nomenclature (Hawthorne et al., 2012). Calculation of tourmaline formulae was based on (O + OH + F) = 31 apfu with no ferric iron, and B and H_2O were calculated by stoichiometry (B = 3 apfu; OH + F = 4 apfu).

3.3. Laser ablation inductively coupled plasma spectrometry (LA-ICP-MS)

Laser ablation ICP-MS analysis of magnetite and biotite was performed with a Coherent GeoLas MV 193 nm laser-ablation system coupled to an Agilent 7900s ICP mass spectrometer at the University of Helsinki. Table 3 lists the settings used for magnetite and biotite. Prior to the final analysis, preliminary tests were done to check the homogeneity of the biotite grains. Most elements were found to be homogeneously distributed, except for the REEs, which we interpret to result from the presence of small and abundant REE-phosphate inclusions. Replicate analyses of the reference materials NIST SRM 610, USGS reference glass GSE-1G, and the natural scapolite standard Sca17 (Seo et al., 2011) were performed to bracket the sample data and to correct for instrumental drift. GSE-1G was selected as external standard for both magnetite and biotite after careful evaluation of the data. Sca17 was used to quantify Cl concentrations in biotite. Data treatment and quantification of the LA-ICP-MS signals were done with the SILLS software package (Guillong et al., 2008). The long-term accuracy of the LA-ICP-MS system was monitored by daily replicate analyses of NIST SRM 612 and was within 5% for most elements.

3.4. Cathodoluminescence imaging

Cathodoluminescence (CL) imaging was performed using a CITL CL8200 Mk5-2 cold-cathode cathodoluminescence system coupled to a Leica DM2700 polarisation microscope equipped with a Peltier-cooled Leica DFC450C high-resolution digital camera at the University of Helsinki. The beam current was set to 0.25 mA and beam voltage at 7.0 kV during all sessions.

4. Results

4.1. Geological and mineralogical evolution of the REE mineralisation in the Olserum-Djupedal district

4.1.1. Main geological features of the Olserum-Djupedal district

The Olserum-Djupedal district comprises three main areas of REE mineralisation: Olserum, Djupedal and Bersummen (Fig. 2). The main ore zone is in Olserum, where dark metasedimentary rocks (Olserum-Djupedal metasediments) containing a set of ESE-WNW to SE-NW-trending, dm-sized veins to metre-wide vein zones with monazite-(Ce), xenotime-(Y) and fluorapatite, are exposed in outcrops within a roughly ESE-WNW-trending zone. These mineralised metasedimentary rocks are

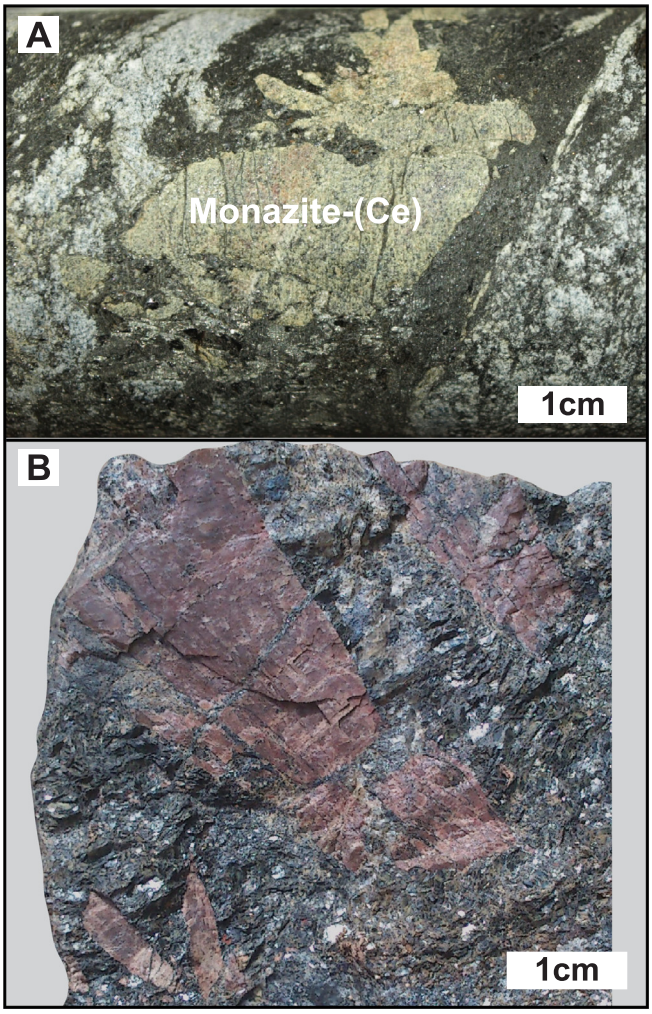

Fig. 3. Hand specimen photos illustrating REE-rich phosphate mineralisation from Olserum-Djupedal with typical coarse-grained crystals of monazite-(Ce) and xenotime-(Y). (A) Large monazite-(Ce) crystal within a biotite-dominated vein in the Olserum area. (B) Large fractured and smaller xenotime-(Y) crystals within a biotite-dominated mineral groundmass in the Djupedal ore assemblages.

exposed in several outcrops at the north-western side of Lake Bersummen as well. Djupedal is located farther inwards from the granite contact, northwest of Olserum (Fig. 2). The REE-phosphate mineralisation is characterised by abundant and large crystals of monazite-(Ce) and xenotime-(Y), which may reach up to 10 cm in length (Fig. 3).

The ore-bearing metasedimentary host rocks are non-foliated to weakly foliated and consist of quartz + plagioclase + biotite ± cordierite ± amphibole (Table 2). Most are grey (Fig. 4A) but some display a reddish-grey colour with increasing plagioclase content. Unmineralised, foliated and folded sillimanite- and cordierite-bearing gneisses are locally present in the south-eastern part of the metasedimentary rocks in Olserum (Fig. 2). The orientation of the main tectonic fabric in these rocks is roughly NW-SE, essentially sub-parallel to the axial trace direction of the regional folds (Gavelin, 1984).

Although the mineralised zones are mainly hosted by metasedimentary rocks, the dominant rock type in the entire Olserum-Djupedal district is alkali feldspar granite (Olserum-Djupedal granite; Fig. 2). This granite is present to the north and south of the exposed ore-bearing metasedimentary rocks in the Olserum area. Observations from drill cores from the Olserum area demonstrate that the metasedimentary rocks are present down to a depth of at least 300 m, but some cores intersect granite at the southern side. Outcrops to the south of the metasedimentary rocks in the Olserum area mainly expose the granite with local occurrences of more readily recognised quartzitic rocks, which are likely part of the Västervik Formation farther south (Fig. 2). The northern contact between the granite and the ore-bearing metasedimentary rocks in the Olserum area dips around 70° to the N and NE. This contact is marked by a transition zone from the more well-preserved metasedimentary rocks through biotite gneisses, intercalated biotite gneisses and granitic to pegmatitic dykes and segregations, and finally to the granite.

The western and eastern extent of the Olserum-Djupedal granite is unknown. The area to the north consists of feldspar-porphyritic granitoids, locally with plagioclase-mantled angular to rounded K-feldspar phenocrysts. In the NE and NW part (Fig. 2), a quartz monzonite is present, which forms part of the quartz monzonite suite (QM; Nolte et al., 2011). These feldspar-porphyritic intrusions are cut by structurally isotropic granitic dykes close to the contact of the Olserum-Djupedal granite. Slightly N to NE of the Djupedal area, metasomatic quartz-plagioclase rocks are present, similar to those described by Hoeve (1974, 1978) (Fig. 2).

4.1.2. Lithology and geochemistry of the Olserum-Djupedal granite

The Olserum-Djupedal granite is normally red, medium-grained and consists mainly of K-feldspar, quartz and biotite with subordinate plagioclase and muscovite, and accessory magnetite, xenotime-(Y), monazite-(Ce), tourmaline (schorl-dravite), fluorite, zircon and fluorapatite. The biotite content of the granite varies significantly (Fig. 4B and C), and rarely forms a foliation in the granite. In particular, along the contact to the metasedimentary rocks in Olserum and Bersummen, a gneissic fabric is present (Fig. 4D). The granite hosts coarse-grained biotite-magnetite schlieren characterised by abundant accessory minerals such as magnetite, monazite-(Ce), xenotime-(Y) and allanite-(Ce) (Table 2). Locally, the granite contains narrow zones where banding is defined by K-feldspar + quartz and fine-grained dark biotite layers. Mafic xenoliths are locally common, as are mafic dykes cross-cutting the granite. Late pegmatitic to granitic dykes and segregations are frequently found in the granite and in the metasedimentary rocks (Fig. 4D and E), and also cross-cutting the REE-bearing veins and vein zones in the Olserum and Bersummen areas. They also seem to transect the fabric in the gneissic granite (Fig. 4D) and the biotite gneiss of the transition zone. The dykes are composed of K-feldspar, albite, quartz and locally muscovite, tourmaline (schorl-dravite), sillimanite, magnetite, monazite-(Ce), xenotime-(Y), uraninite, columbite-(Fe) and fluorapatite. Rarely, the tourmaline occurs as symplectitic intergrowths with quartz (Fig. 4E).

Geochemically, the Olserum-Djupedal granite is ferroan (Frost et al., 2001), calc-alkalic to alkali-calcic, peraluminous and exhibits high Si

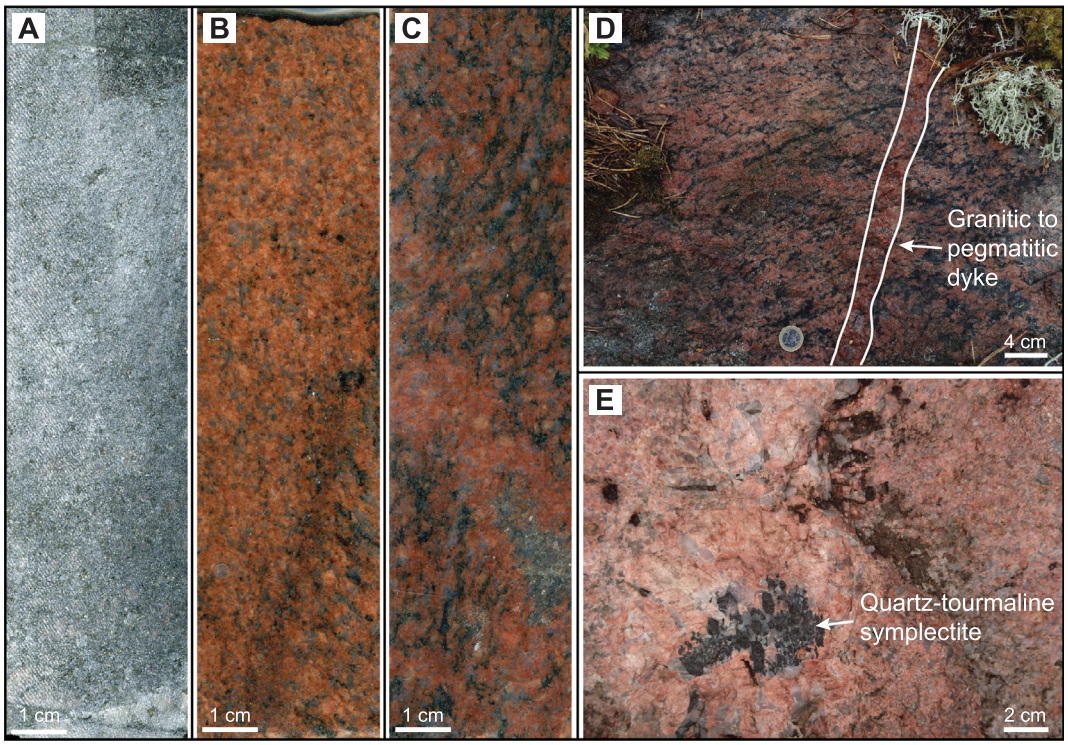

Fig. 4. Examples of rock types and key structures of the Olserum-Djupedal district. (A) Drill core slab showing the dominant grey metasedimentary rocks that host the REE mineralisation. (B) Drill core slab of biotite-poor Olserum-Djupedal granite. (C) Drill core slab of a biotite-rich Olserum-Djupedal granite. (D) Bersummen: Granitic to pegmatitic dykes cross-cutting the main fabric in the gneissic granite. (E) Bersummen: Pegmatitic segregations within the granite. Tourmaline and quartz form a symplectitic intergrowth.

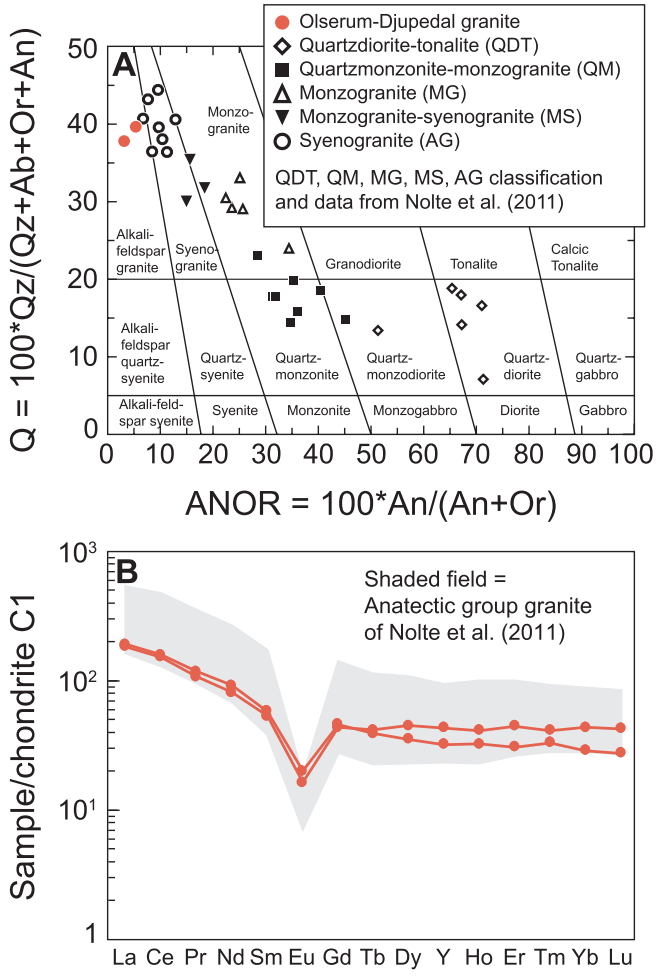

Fig. 5. Diagrams displaying the composition of the Olserum-Djupedal granite in (A), CIPW-normalised Q versus ANOR diagram (Streckeisen and LeMaitre, 1979), and (B), REE distribution diagram normalised to chondrite C1 (normalisation after Sun and McDonough, 1989).

(about 76 wt% SiO_2) and $Na_2O + K_2O$ (8.1–8.9 wt%) contents, and plots in the field of alkali feldspar granite in the Q-ANOR CIPW-normalised diagram (Fig. 5A; representative whole-rock geochemical data are available in the online data repository). It is enriched in Cs, Rb and Ba. The REE distribution diagram shows a LREE-enriched pattern with $(La/Yb)_N$ at 4 to 7 (normalised to C1 chondrite; Sun and McDonough, 1989), and with a negative Eu anomaly (Fig. 5B). The P content is low (0.04–0.07 wt% P_2O_5) and the ΣREE + Y content is around 300 ppm, which is overall lower than that of other granitoids and syenitoids in the Västervik region (Nolte et al., 2011). The REE-bearing minerals are typically concentrated in the biotite-magnetite schlieren. The granite has a higher Th content (22–27 ppm) than igneous rocks from other granitoid and syenitoid suites in the Västervik region, whereas the U concentration (about 5 ppm) is similar to the other suites (Nolte et al., 2011). The Zr concentration is rather high (about 230 ppm), but generally lower than those of rocks from the other suites. The alkali feldspar granite of the Olserum-Djupedal district therefore corresponds to the anatectic granite suite (AG), which likely formed by low-pressure melting of the Västervik Formation at moderately shallow (c. 15 km) crustal depths in an extensional to transtensional tectonic setting (Nolte et al., 2011; Kleinhanns et al., 2015).

4.1.3. Mineralogical and field relations of the REE mineralisation in the Olserum-Djupedal district

The REE mineralisation in the Olserum and Bersummen areas is mostly hosted by the metasedimentary rocks and partly by biotite gneisses in the transition zone and the Olserum-Djupedal granite. In the Djupedal area, however, REE mineralisation is hosted by larger, partly migmatised metasedimentary bodies, probably xenoliths, enclosed in the granite (Fig. 2).

In the Olserum and Bersummen areas, the REE mineralisation mostly occurs as up to dm-wide veins in the metasedimentary rocks and in the granite adjacent to the contact with the metasedimentary rocks. The veins are present as individual veins, or as sets of interconnected veins, which primarily consist of biotite, quartz, magnetite, fluorapatite, xenotime-(Y), monazite-(Ce) and subordinate cordierite, ilmenite and (REE,Y,Th,U,Ca)-(Nb,Ta)-oxide(s) (Fig. 6A and B). In Olserum, locally up to several metres wide vein zones are present. One of these is exposed in the main mineralised outcrop at Olserum (Fig. 2) and others have been intersected in the drill cores. The vein zones differ from the veins in that they contain abundant amphibole (gedrite) and lack clearly discernible individual or interconnected veins. They are characterised by metres-wide, continuous zones along strike with gedrite, biotite and magnetite, and carry abundant and coarser-grained xenotime-(Y), monazite-(Ce) and fluorapatite (Fig. 6C and D). The vein zones are generally associated with the highest REE ore grades (labelled as BMSR; Reed, 2013) and are typically also richer in magnetite. Locally, the REE-bearing veins principally lack magnetite (e.g., in Bersummen) whereas in other places, magnetite dominates over biotite. The REE-bearing veins and vein zones are oriented roughly ESE-WNW to SE-NW, i.e., conformable with the overall orientation of the main fabric in the metasedimentary rocks. Granitic to pegmatitic dykes frequently cross-cut the ores in the metasedimentary rocks, both in the Olserum and Bersummen areas (Fig. 6D and E).

Drill core observations from the Olserum area show that the REE-phosphates and fluorapatite are also present in biotite-dominated veins in the biotite gneisses in the transition zone, and these sometimes coalesce with the gneissic fabric. REE-phosphates and fluorapatite are also present within individual or interconnected biotite-dominated veins in the granite proximal to the contact. Close to these granite-hosted veins, the granite typically displays an increased biotite content. The granite-hosted veins are locally exposed in outcrops (Fig. 6F and G), and are surrounded by a grey alteration zone mainly composed of biotite, quartz and altered feldspar. Similar alteration zones containing disseminated xenotime-(Y), monazite-(Ce) and minor zircon locally cut the fabric in the gneissic granite (Fig. 6H). The lateral extent of all REE-bearing veins is mostly difficult to delineate because of the sporadic and incomplete nature of the exposures. However, the veins can, in some cases, be traced for several metres along strike, beyond which they gradually thin and finally pinch out.

In the Djupedal area, the metasedimentary rocks are only sparsely exposed within a small, topographically low area, which is otherwise dominated by the Olserum-Djupedal granite. The exposures of the metasedimentary rocks are typically very limited and the geological relation between them and the granite is not fully understood. The metasedimentary rocks are present as several metres large, partly migmatised bodies surrounded by the granite, and the Djupedal area may represent a migmatitic contact aureole of the granite. These bodies are also intersected in some drill cores from the Djupedal area, which were drilled near the exposures of the sedimentary rocks close to the iron mines (Fig. 2).

The metasedimentary rocks in Djupedal are locally rather well-preserved, with only patchy to slightly stromatic migmatitic appearance. In such pristine exposures, around 1 dm wide, coarse-grained biotite veins, and more irregular and variably thick biotite-rich patches with xenotime-(Y), fluorapatite and minor monazite-(Ce) are usually also well-preserved (Fig. 7A). These veins are oriented roughly in an N-S direction, which is different from the Olserum and Bersummen areas. In migmatitic melt-dominated exposures, the melt veins (neosome/leucosome) consist of K-feldspar and quartz with local melanocratic bands of biotite, quartz and subordinate muscovite. These melt veins

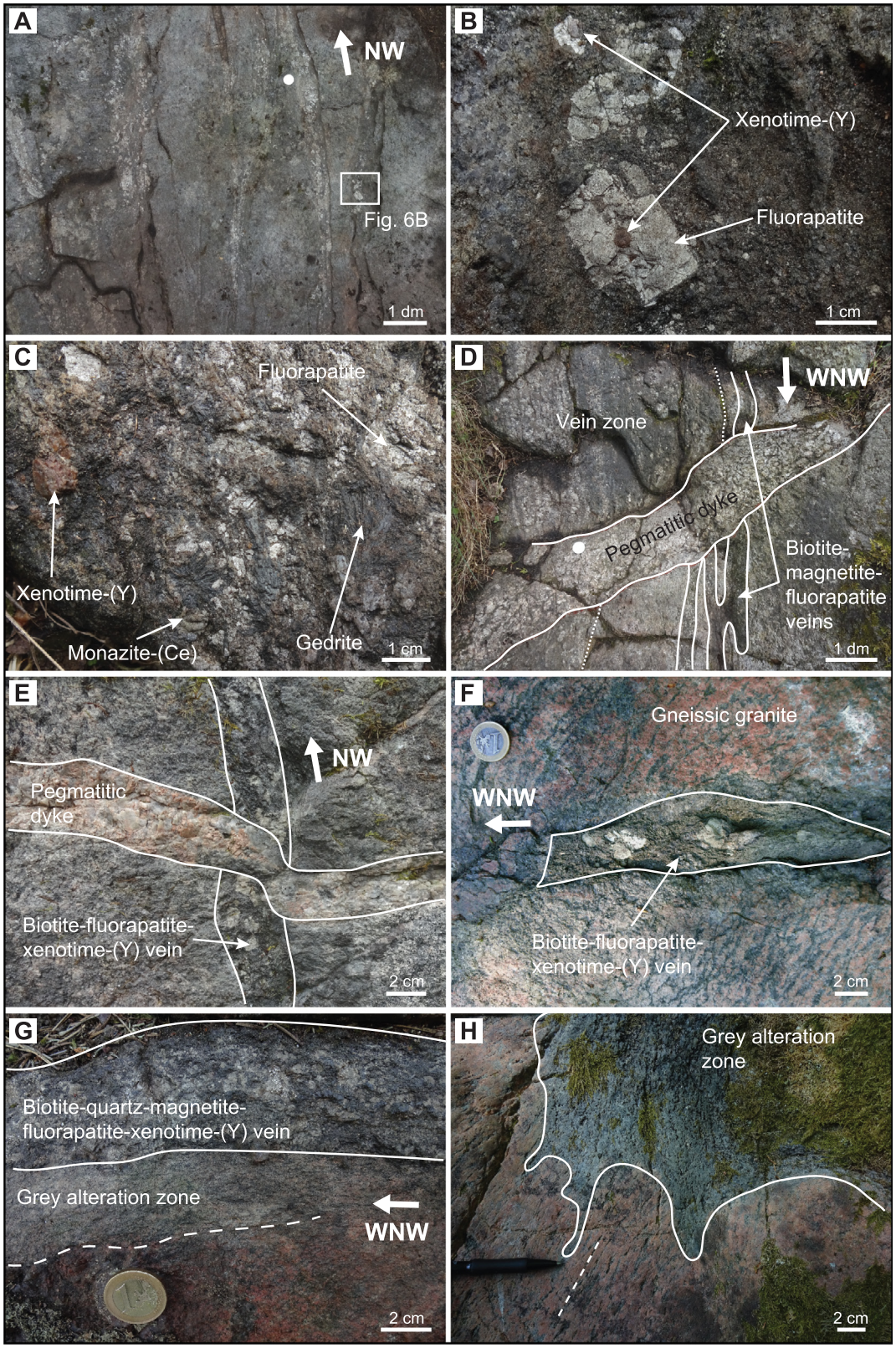

Fig. 6. Key structures and field relationships in the Olserum and Bersummen areas. (A) Bersummen: Set of interconnected REE-bearing veins containing fluorapatite, monazite-(Ce) and xenotime-(Y) oriented approximately NW-SE. (B) Bersummen: Close-up of the REE-bearing veins shown in (A). Coarse-grained fluorapatite intergrown with xenotime-(Y). (C) Olserum: Amphibole (gedrite) rich vein zone with coarse-grained xenotime-(Y), monazite-(Ce), fluorapatite, magnetite, biotite and quartz. (D) Olserum: Vein zone and veins cut by a granitic to pegmatitic dyke. Fluorapatite-biotite-dominated veins are present in the centre and at the right-hand side of the photograph. These REE-bearing veins and the vein zone are displaced at the contact with the dyke. (E) Bersummen: An individual vein composed of biotite-fluorapatite-xenotime-(Y) cross-cut by a pegmatitic dyke (oriented horizontally). (F) Bersummen: Discontinuous REE-bearing vein in the granite displaying a clear fabric. (G) Olserum: A biotite-magnetite-quartz-fluorapatite-xenotime-(Y) vein within the granite close to the contact between the metasedimentary rocks and the granite. Closer to the vein, the granite has a greyer colour (weak alteration). (H) Olserum: Ore-related alteration zones cutting the main fabric (white broken line) of the gneissic granite. These zones host hydrothermal xenotime-(Y), monazite-(Ce) and zircon.

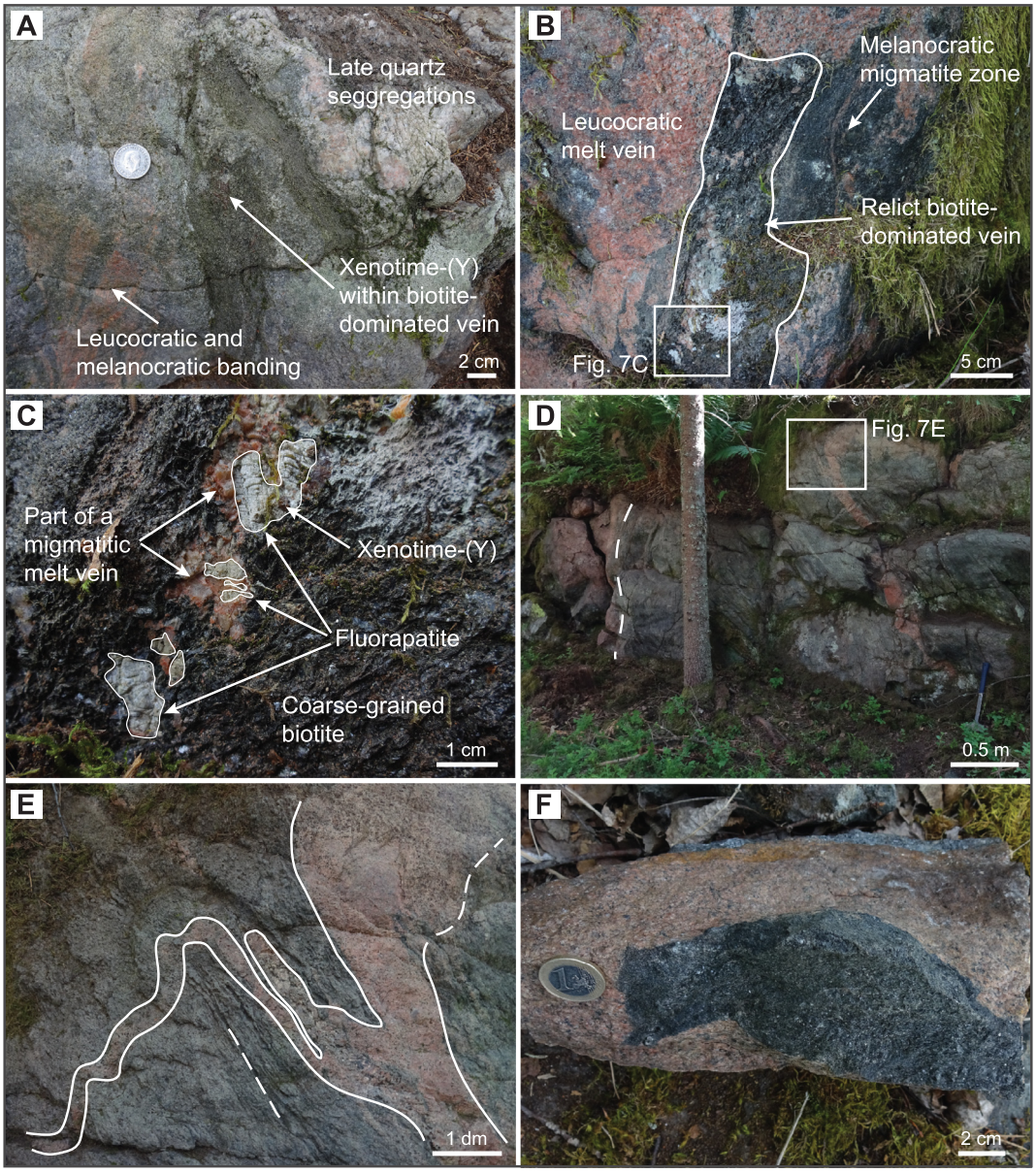

Fig. 7. Key structures and field relationships in the Djupedal area. (A) Well-preserved set of REE-mineralised veins and aggregates of mostly coarse-grained biotite with large xenotime-(Y) crystals. Faint leucocratic and melanocratic banding are visible in the lower left corner. Late quartz segregations are present in the upper right part of the photo. (B) Migmatitic melt-dominated part of the same outcrop as shown in (A). Leucocratic migmatitic melt veins of K-feldspar and quartz, and melanocratic zones enclose relicts of a fluorapatite-bearing vein. (C) Close-up of the area highlighted with a white frame in (B). Patches of a migmatitic melt vein composed of K-feldspar and quartz enclose and intrude into fractures (centre) of fluorapatite and minor xenotime-(Y). (D) Overview of a large ore-bearing metasedimentary body within the granite. A larger granitic dyke extends from the metasedimentary rock into the main granite body. The dashed line marks the contact with the granite. (E) Close-up of the area highlighted by a white frame in (D). A granitic dyke cross-cutting the fabric (represented by the dashed line) in the ore-bearing metasedimentary body. (F) Inclusion or patch of a relict coarse-grained biotite-dominated vein in the granite. Some similar inclusions or patches contain large fluorapatite crystals.

have intruded, or cross-cut the phosphate-bearing biotite veins and patches, and in some cases, even enclosed the fluorapatite crystals and may occur within fractures of them (Fig. 7B and C).

Locally in the Djupedal area, granitic dykes extend from the metasedimentary bodies, where they cross-cut the foliation and the mineralised veins and patches, into the granite (Fig. 7D and E). Inclusions or patches of coarse-grained biotite with rare fluorapatite crystals are also locally found within the granite (Fig. 7F). These field relations suggest that the ore-bearing metasedimentary rocks locally underwent anatexis and produced some volume of the granite in the area. The studied ore samples from the Djupedal area represent material from the two main, old open pits from the days of magnetite mining. These samples are characterised by up to dm-sized, extensively fractured crystals of xenotime-(Y), monazite-(Ce) and fluorapatite within a groundmass of mainly coarse-grained biotite, quartz, magnetite, muscovite and cordierite. Locally, allanite-(Ce) – ferriallanite-(Ce) and other Ca-bearing minerals occur, including tourmaline (uvite-feruvite), clinozoisite and a later generation of fluorapatite (Andersson et al., 2018). Other minerals exclusively found in the Djupedal mineralisation are bastnäsite-(Ce), scheelite and ferberite (Table 2). The immediate host rock to these open pit mines (now water-filled) consists of grey metasedimentary rocks surrounded by the granite, and the pits probably targeted similar ore-bearing metasedimentary bodies as exposed in outcrops in the area.

Several of the old iron mines in the Olserum-Djupedal district

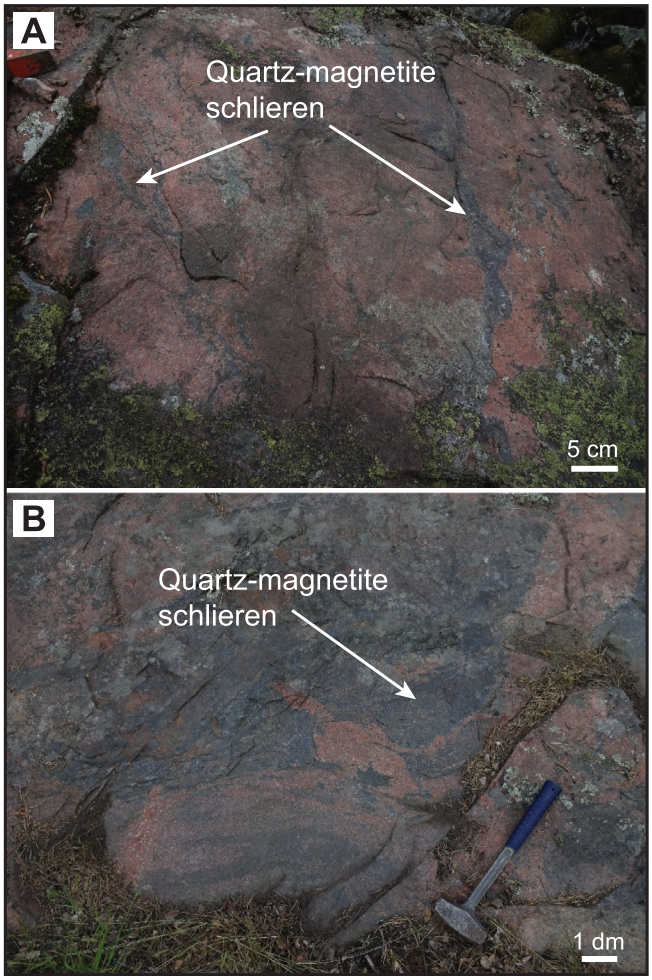

Fig. 8. Field relationships of intra-granitic magnetite ores in the Olserum-Djupedal district. (A) Quartz-magnetite schlieren in an alkali feldspar dominated granite. (B) More complex relationship between the quartz-magnetite schlieren and the granite.

(Fig. 2; e.g., Källhagen) have mainly mined intra-granitic accumulations of quartz-magnetite schlieren- or biotite-magnetite schlieren-hosted ores (Fig. 8). The quartz-magnetite schlieren ores contain partly martitised magnetite with abundant intergrown monazite-(Ce) hosting small xenotime-(Y) grains. The relative timing of these magnetite ores in relation to the main REE-bearing veins is however uncertain at present, but they are assumed to be coeval with the REE mineralisation in the metasedimentary rocks. This is because in addition to the similar mineralogy of schlieren-type ores and the metasediment-hosted REE ore, the schlieren-type ores in Olserum are markedly concentrated along the contact between the Olserum-Djupedal metasedimentary rocks and the Olserum-Djupedal granite, but systematically farther inwards towards the granite centre.

4.1.4. Occurrences of quartz-plagioclase rocks and associated Na ± Ca metasomatism

In an area 400 m north of the Djupedal mineralised area (Fig. 2), a white quartz-plagioclase-dominated rock is present (Fig. 9A). The field relationships between this rock and the Olserum-Djupedal granite are ambiguous. An Olserum-Djupedal-like granite is locally present as inclusions within the quartz-plagioclase rocks. In other places, red thin granitic bands emanating from the granite cut the quartz-plagioclase rock, but are themselves transected by thicker aplitic dykes, which also displace the thinner bands. Closer to the boundary between the Olserum-Djupedal granite and the porphyritic granitoids (Fig. 2), this quartz-plagioclase rock shows a gradual contact to a quartz monzonite (QM suite), and both rocks are cut by aplitic dykes.

The quartz-plagioclase rock is mainly composed of coarse-grained quartz and plagioclase and fresh K-feldspar is locally present. CL imaging shows that K-feldspar is largely replaced by plagioclase (Fig. 9B). This plagioclase exhibits a yellow to yellowish-brown luminescence colour, and preliminary EDS analyses indicate compositions ranging from albite to oligoclase. In transmitted light, this plagioclase is transparent but commonly exhibits a light to dark brown dusty appearance, possibly resulting from alteration affecting the plagioclase after the initial replacement. This plagioclase is also intergrown with quartz in a myrmekitic texture (Fig. 9C). Primary K-feldspar frequently exhibits perthite flames of plagioclase with a darker blue to purple luminescence colour (Fig. 9C).

Niobium-bearing rutile and ilmenite are both common as accessory minerals in the quartz-plagioclase rock and are typically replaced by titanite ± rutile ± hematite (Fig. 9D). Zircon is also rather common, and displays growth zoning, locally with Ca-enriched zones. The other minerals identified in this rock are clinozoisite, pyrophanite ($MnTiO_3$), a columbite-tantalite group mineral (probably columbite-(Fe)) and a Th-rich phase belonging to the cheralite-huttonite-monazite series (Linthout, 2007). The appearance and mineralogy of the quartz-plagioclase rock are very similar to the quartz-plagioclase rocks described by Hoeve (1974) in the Västervik region, which were interpreted as the product of Na ± Ca metasomatism.

More detailed CL imaging of feldspar from the Olserum-Djupedal granite, and from the leucocratic melt veins in Djupedal reveals textural features similar to those from the quartz-plagioclase rock. K-feldspar from the Olserum-Djupedal granite display a turquoise to light blue colour in CL. It is also perthitic, where plagioclase occurs as flames and patches (Fig. 9E). Plagioclase often seemingly encloses some K-feldspar too, possibly indicating replacement of K-feldspar. This type of plagioclase mostly has a dark blue to purple luminescence colour with reddish rims, and rarely displays a lighter purplish colour. Preliminary EDS analyses suggest compositions close to pure albite. More Ca-rich plagioclase, with the same yellow to brownish-yellow luminescence colour, as in the quartz-plagioclase rocks, mostly replaces the albitic plagioclase, but also the perthitic K-feldspar (Fig. 9F). This replacement is more developed proximal to the REE-bearing veins, but does also occur locally within the chemically most evolved granite, distal to these veins.

4.2. Petrography of the ore-bearing assemblages in the Olserum-Djupedal REE mineralisation

A characteristic feature of the REE ore zones in the Olserum-Djupedal district is that the primary REE-bearing minerals monazite-(Ce), xenotime-(Y), fluorapatite and minor (Y,REE,U,Fe)-(Nb,Ta)-oxides are variably fractured and recrystallised. The gangue (vein groundmass) minerals infill these fractures and enclose the REE-bearing minerals (Fig. 10A and B). The gangue minerals mainly comprise biotite, amphibole (gedrite and anthophyllite), magnetite and quartz, while ilmenite, cordierite, andalusite, white mica or muscovite, tourmaline (uvite and dravite-schorl), chlorite and plagioclase are only locally abundant (Fig. 10B and C).

Biotite is typically present as coarse-grained, sometimes up to 1 cm-sized platy crystals, infilling and enclosing the fractured REE-bearing minerals. In granite-hosted veins, and in veins close to the granite contact in the Olserum area, biotite is mostly associated with magnetite intergrown with monazite-(Ce) and xenotime-(Y) (Fig. 10D). Biotite rarely exhibits kink bands. Magnetite is otherwise mostly present in the REE ore zone in the vein groundmass as euhedral to anhedral grains, or larger anhedral aggregates closely associated with ilmenite. Metasediment-hosted magnetite contains abundant exsolution lamellae of an Al-rich spinel phase. In contrast, magnetite hosted by granitic rocks, including the schlieren ores in the granite, lacks these exsolution

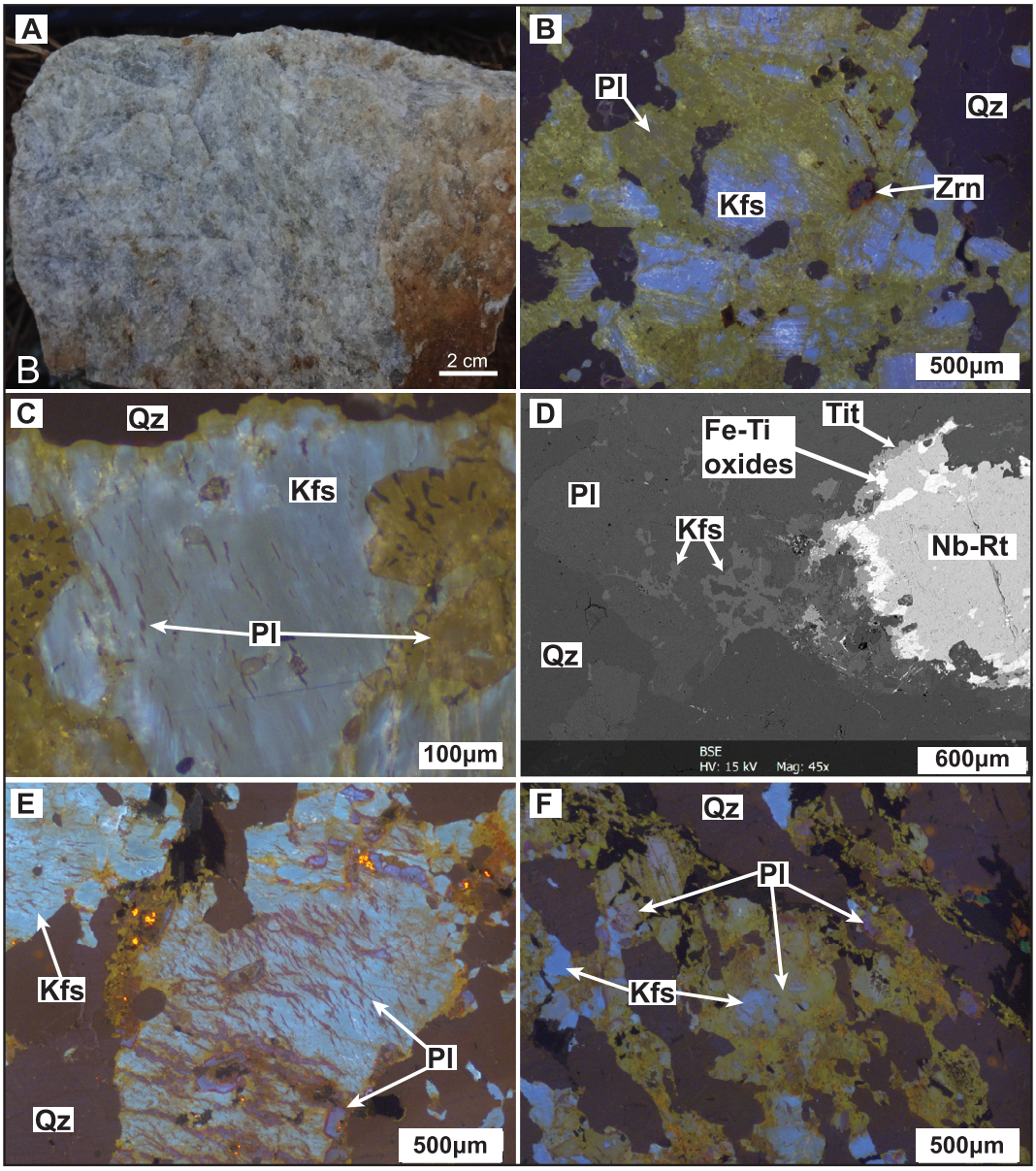

Fig. 9. Hand specimen, backscattered electron (BSE) and CL images illustrating the occurrence of metasomatic quartz-plagioclase rocks and associated metasomatism in the Olserum-Djupedal district. (A) White quartz-plagioclase rock in Djupedal. (B) Quartz-plagioclase rock: CL image showing the replacement of light blue K-feldspar by yellow-brown plagioclase (albite to oligoclase in composition) with some accessory zircon. (C) Quartz-plagioclase rock: CL image illustrating light blue K-feldspar partially altered by yellow-brown plagioclase with quartz as a myrmekitic intergrowth, and with dark blue-purple albitic flame perthite. (D) Quartz-plagioclase rock: BSE image depicting the replacement of Nb-rutile by titanite and Fe-Ti oxides, and of K-feldspar by plagioclase. (E) Olserum-Djupedal granite: CL image showing light blue K-feldspar with dark-purple flame and patchy perthite of albitic composition. The plagioclase normally exhibits a reddish rim. Sample of the chemically most primitive granite. (F) Olserum-Djupedal granite: CL image displaying yellow-brown plagioclase mainly replacing dark blue-purple and brighter purple plagioclase and also some light blue K-feldspar (centre). Also shown are minor green xenotime-(Y) together with weakly luminescent monazite-(Ce) with pleochroic haloes (right). Mineral abbreviations: Kfs: K-feldspar; Nb-Rt: Nb-bearing rutile; Pl: plagioclase; Qz: quartz; Tit: titanite; Zr: zircon. (For interpretation of the references to colour in this figure legend, the reader is referred to the web version of this article.)

lamellae. Magnetite is commonly replaced by chlorite ± calcite, or martitised (oxidised to hematite) late in the paragenetic sequence. Martitisation is most widespread in granite-hosted magnetite, and occurs only locally in the REE ore zone in the Olserum and Djupedal areas.

Amphibole mostly forms larger intergrowths of crystals, or radial aggregates, and some individual crystals exhibit euhedral outlines towards biotite. Amphibole is occasionally associated with cordierite as an alteration product (Fig. 10E), where it locally forms a symplectitic intergrowth with an Al-silicate, most likely andalusite, in the metasedimentary host rock or rarely in the REE ore zone in the Olserum area.

Cordierite appears within the vein groundmass, primarily in the Djupedal area (Fig. 10C), sometimes also containing smaller inclusions of the REE-phosphates. Cordierite exhibits distinct breakdown textures (e.g., Fig. 10E), and minerals formed by this process are quartz, andalusite or a quartz-andalusite symplectite, staurolite, amphibole, biotite, muscovite, as well as additional phases typical of “pinite” alteration. Andalusite is locally present along rims of biotite (Fig. 10D) and does, together with biotite, plagioclase, quartz, magnetite, muscovite and secondary monazite-(Ce) and xenotime-(Y), locally enclose primary fluorapatite (Fig. 10F) or fill fractures in primary fluorapatite.

Muscovite is only a minor mineral in the Olserum area and is mainly present in the granite-hosted veins. In the Djupedal area, muscovite is a more common gangue mineral present within the vein groundmass of

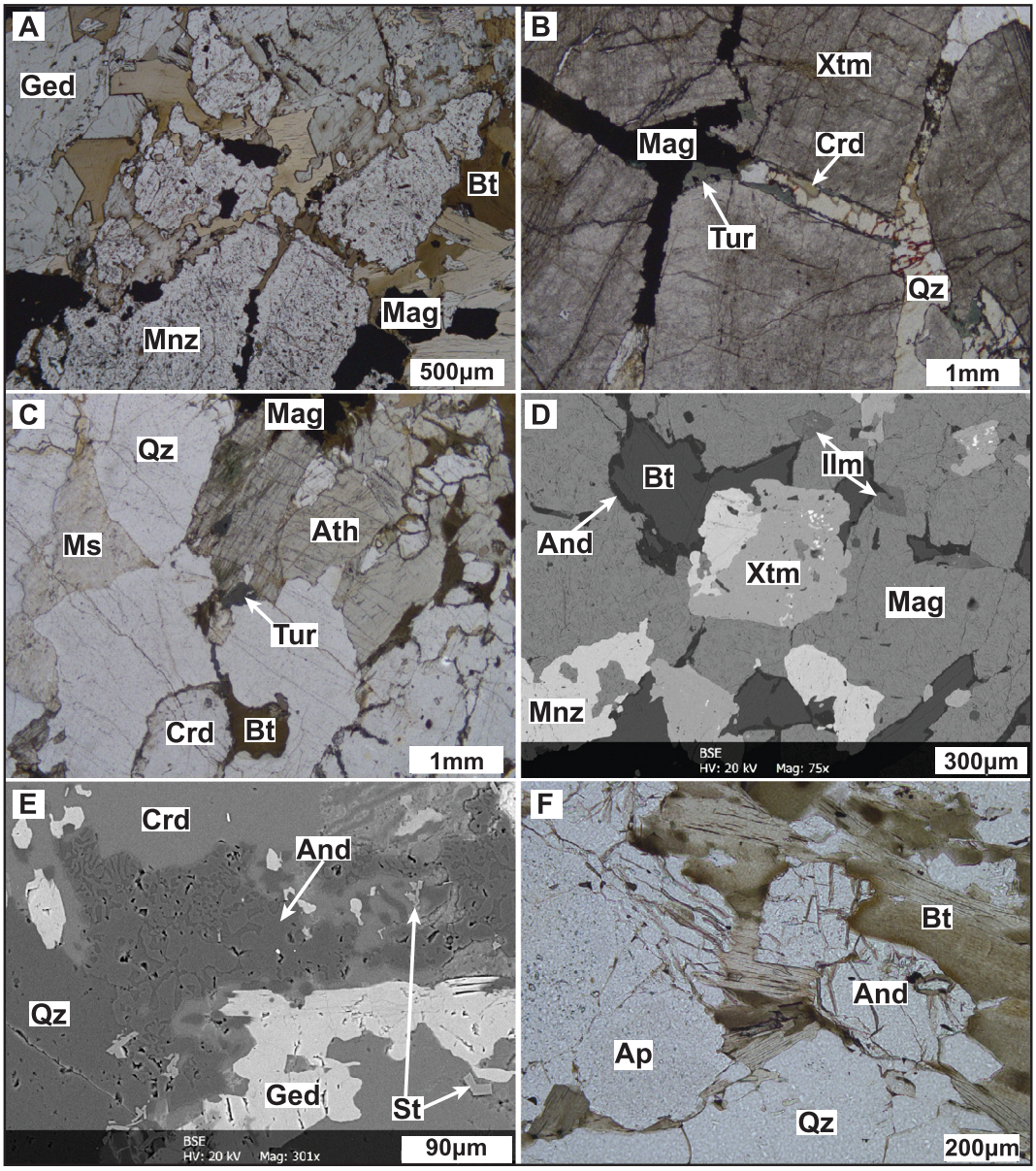

Fig. 10. Photomicrographs and BSE images displaying the main petrographic features of the REE ore assemblages in the Olserum-Djupedal REE mineralisation. (A) Olserum: Euhedral and fractured primary monazite-(Ce) crystal enclosed by biotite, gedrite and magnetite. (B) Djupedal: Euhedral and fractured primary xenotime-(Y) crystal with infill of magnetite, tourmaline, cordierite and quartz. (C) Djupedal: Mineral groundmass in Djupedal, consisting of anthophyllite, quartz, cordierite, muscovite, biotite, magnetite and tourmaline. (D) Olserum: Intergrown xenotime-(Y) and monazite-(Ce) with magnetite together with ilmenite and biotite. Andalusite forms as rims on biotite. (E) Djupedal: Breakdown of cordierite with andalusite-quartz symplectite, gedrite and staurolite as breakdown products. (F) Olserum: Locally formed andalusite together with biotite and quartz in the surrounding vein groundmass of primary fluorapatite crystals. Mineral abbreviations: And: andalusite; Ap: fluorapatite; Ath: anthophyllite; Bt: biotite; Crd: cordierite; Ged: gedrite; Ilm: ilmenite; Mag: magnetite; Mnz: monazite; Ms: muscovite; Qz: quartz; St: staurolite; Tur: tourmaline; Xtm: xenotime.

fractured primary REE-bearing minerals. This muscovite occasionally forms a symplectitic texture with quartz, which may represent a breakdown product of earlier high-grade minerals. Tourmaline is also limited to the REE ore zone in the Djupedal area and is there associated with allanite-(Ce), magnetite, cordierite, biotite and muscovite within the vein groundmass of the fractured REE-bearing minerals. Tourmaline also, albeit rarely, forms symplectitic intergrowths with quartz.

Chlorite (sensu lato) is only a minor primary component in the REE ore zone in the Olserum area. Chlorite is mainly present later in the paragenetic sequence as an alteration product of biotite, amphibole, magnetite or allanite-(Ce) – ferriallanite-(Ce) in both the REE ore zone and within the host metasedimentary and granitic rocks.

4.3. Mineral chemistry of the major gangue minerals

4.3.1. Biotite

The analysed biotite falls into the compositional quadrilateral of annite $[K_2Fe_6(Si_6Al_2O_{20})(OH,Cl,F)_4]$, phlogopite $[K_2Mg_6(Si_6Al_2O_{20})(OH,Cl,F)_4]$, siderophyllite $[K_2Fe_5Al(Si_5Al_3O_{20})(OH,Cl,F)_4]$ and eastonite $[K_2Fe_5Al(Si_5Al_3O_{20})(OH,Cl,F)_4]$ (Fig. 11). Ore-associated biotite from the veins and vein zones in the metasedimentary rocks in the Olserum area is dominantly phlogopite, and becomes increasingly Fe- and Al-rich towards the contact with the granite. Ore-associated biotite in the metasedimentary rocks in the Djupedal and Bersummen areas is also Mg-dominant and straddles the phlogopite-eastonite border. Biotite from the granite-hosted veins and biotite in the granite is Fe-rich,

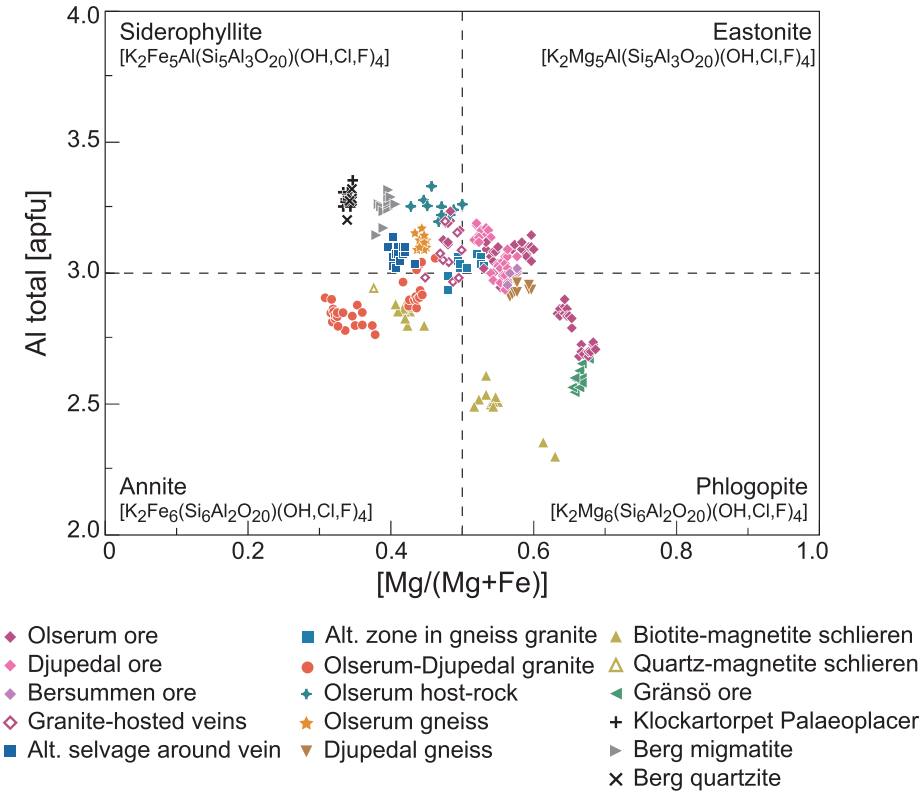

Fig. 11. Diagram illustrating major element chemistry of biotite. Plot of the total Al (apfu) versus the Mg/(Mg + Fe) ratio.

with Mg/(Mg + Fe) typically below 0.5. Notably, ore-associated biotite in the metasedimentary rocks is Na-rich, reaching almost 1 wt% Na_2O (or 0.3 apfu Na; Fig. 12A). The Na content decreases with increasing Al content and increases with increasing Mg/(Mg + Fe) and Si content. Therefore, the most Na-rich biotite plots as phlogopite in the Al versus Mg/(Mg + Fe) diagram (Fig. 11). The Na content gradually decreases in biotite from the REE-bearing veins with proximity to the granite contact in the Olserum area. Biotite from the granite-hosted REE-bearing veins exhibit a Na concentration similar to biotite from the granite (< 0.2 wt % Na_2O). Biotite from Gränsö also plots as phlogopite, but, in contrast to ore-associated biotite from the Olserum-Djupedal district, is low in Na (< 0.2 wt% Na_2O).

The Ti content of all ore-associated biotite in the metasedimentary rocks is low, below 1.5 wt% TiO_2 (Fig. 12B). By contrast, biotite hosted in the granitic rocks is substantially richer in Ti, ranging from 1.6 to 2.9 wt% TiO_2, excluding biotite associated with minor alteration zones around the granite-hosted veins. Biotite associated with these alteration zones has a green colour in thin section, in contrast to the dark brown colour of biotite found elsewhere in the studied mineralisation. The green biotite probably represents biotite re-equilibrated at lower temperatures (Henry et al., 2005).

Ore-associated biotite in the metasedimentary rocks, and in the host metasedimentary rocks themselves, has low Rb concentration (< 700 ppm), translating into a high K/Rb ratio (Fig. 12A–H). Moreover, the Rb content in ore-associated biotite increases gradually towards the granite contact in the Olserum area. Biotite from the granite-hosted veins exhibits similar Rb concentration as biotite of the granite that hosts these veins.

Three samples of the Olserum-Djupedal granite display a clear trend of increasing Rb concentrations (and decreasing K/Rb) in biotite from the granite hosting the REE-bearing veins at the contact, to biotite in the granite distal to this contact, and then to biotite from a granite sample farther away from this contact. This trend can be interpreted in terms of progressive magmatic evolution of the granitic system. Comparable trends are also clearly shown by Cs, Mn and Tl, which all increase towards the chemically most evolved granite (Fig. 12C–E). Cobalt, Cr, Ga, Sn and Zn (Fig. 12F) also show a general increase with chemical evolution of the granite, but the trend is not as clear as for the other elements. The concentrations of Na (Fig. 12A) and Nb decrease with decreasing K/Rb. Barium, Fe, Li, Sc and Sr first increase, and then they decrease again towards the most evolved granite (Fig. 12G). A reversed trend (i.e., first a decrease followed by an increase) is shown by Mg, Ni, Pb, Ta, V and W (Fig. 12H). Ore-associated biotite proximal to the granite contact in the Olserum area generally has higher concentrations of Ba, Mn, Nb, Sc, Sn, Ta, Ti, V, W and Zn relative to ore-associated biotite distal to this contact. Conversely, Cs and Ni are lower in ore-associated biotite closer to the granite contact. Taken together, the REE ore-associated biotite in all areas generally displays lower or slightly overlapping concentrations of most trace elements compared to biotite in the granites and granite-hosted veins. The exceptions are Ni, Pb, Sc, Sr, V and W, which are higher in biotite associated with the REE mineralisation.

Biotite from Gränsö is markedly enriched in Cr, Ni and Mo relative to ore-associated biotite in the Olserum-Djupedal district. Biotite from the palaeoplacer deposit at Klockartorpet and biotite from the quartzite of the migmatite occurrence at Berg exhibits a similar major element mineral chemistry and displays high concentrations of Cr, Ti and V. Likewise, biotite from the migmatitic melt veins in Berg has high contents of Cr, Ti and V.

Biotite, together with fluorapatite, is the major carrier of halogens in the REE ore zone in the Olserum-Djupedal district. The measured F concentration in biotite ranges from around 0.6 up to 3.5 wt% in the ore assemblages. The F content of biotite from the granite is between 1.0 and 3.1 wt% F. The Cl content in biotite ranges from 0.15 to 0.75 wt% in the ore assemblages, and reaches up to 1.2 wt% in the most Fe-rich biotite from the granite. Because of crystal-chemical energetic couplings commonly referred to as F-Fe avoidance and Mg-Cl avoidance, biotite incorporates more Cl with increasing Fe concentration, and more F with increasing Mg (Ramberg, 1952; Munoz, 1984). Therefore, the Cl and F concentrations should both correlate with the Mg/

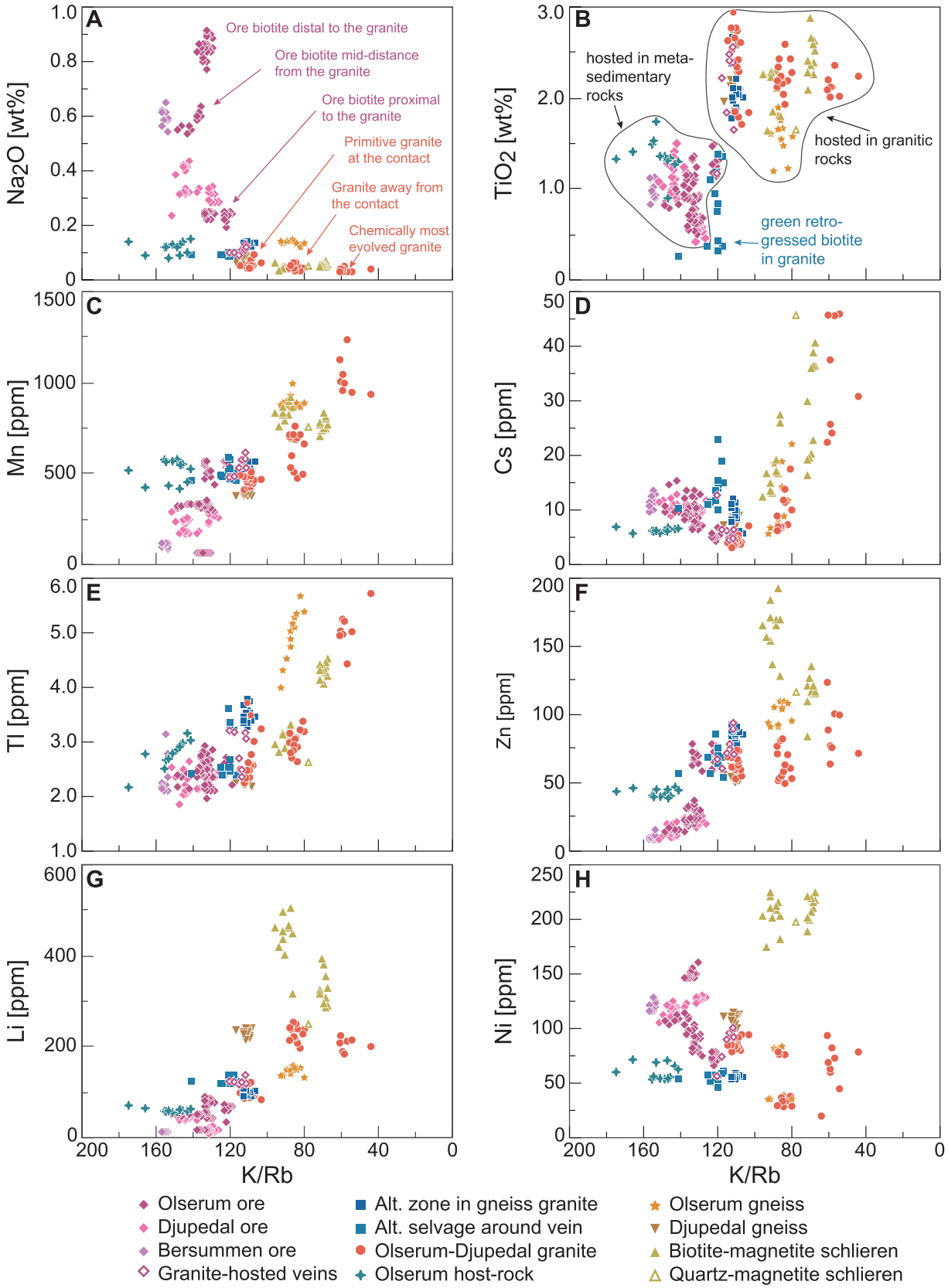

Fig. 12. Diagrams of representative major and trace element concentrations in biotite from the Olserum-Djupedal district plotted against the K/Rb ratio. (A) Na_2O. (B) TiO_2. (C) Mn. (D) Cs. (E) Tl. (F) Zn. (G) Li. (H) Ni.

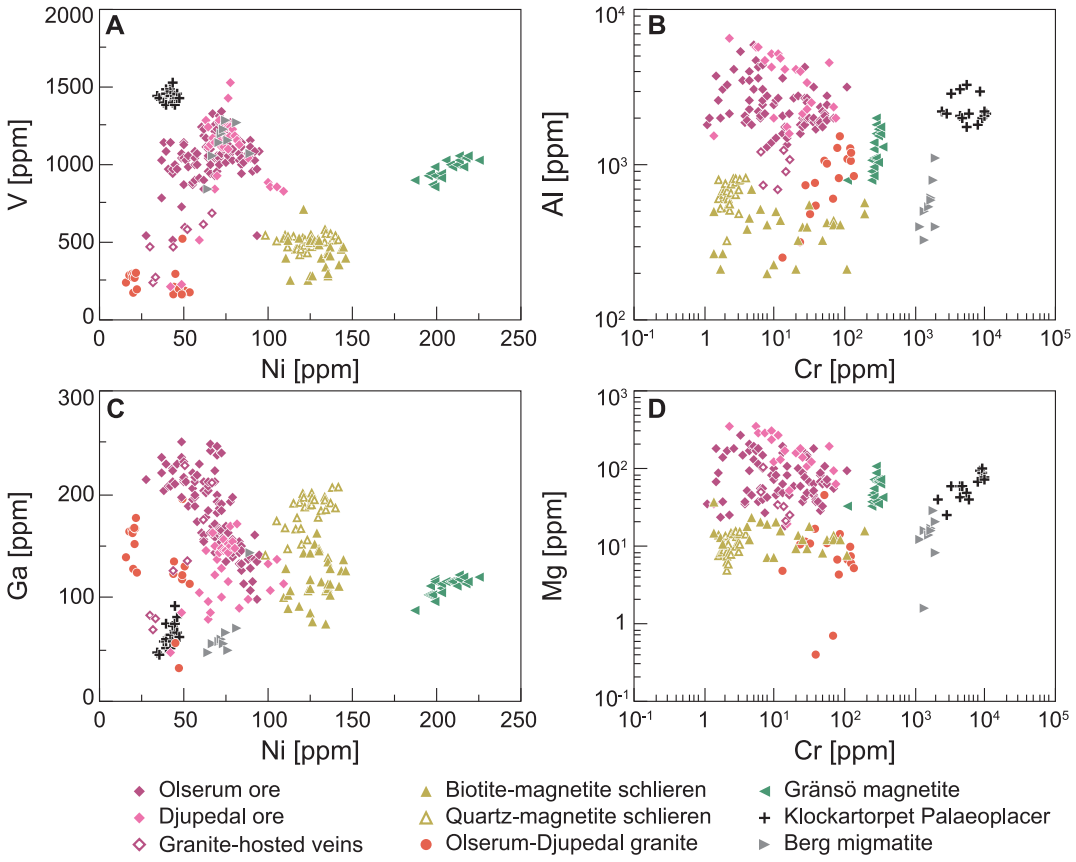

Fig. 13. Variation diagrams illustrating the trace element chemistry of magnetite from the Västervik region. (A) V against Ni. (B) Al against Cr. (C) Ga against Ni. (D) Mg against Cr.

(Mg + Fe) ratio. For biotite in the Olserum-Djupedal district, the data show that this is the case for Cl, which increases with decreasing Mg/(Mg + Fe) ratio. Because the Fe content in biotite increases with proximity to the granite contact in the Olserum area, the Cl concentration also increases towards this contact. The data show that F is not as strongly correlated with the Mg/(Mg + Fe) ratio.

4.3.2. Magnetite

Magnetite is abundant in the REE-bearing veins and vein zones in the Olserum-Djupedal district. EPMA analysis of the magnetite shows that it is almost pure with only a minor Al content. Only magnetite from the Klockartorpet palaeoplacer contains significant concentrations of another element, namely Cr.

Metasediment-hosted magnetite in the REE-bearing assemblages of both the Olserum and Djupedal areas is compositionally very similar. It is comparably higher in V (average: 1060 ± 190 ppm), Al (average: 2760 ± 1180 ppm), and Mg (average: 110 ± 75 ppm) than magnetite hosted in granitic rocks in the Olserum-Djupedal district. The concentrations of Ti (average: 750 ± 620 ppm) and Ga (average: 170 ± 40 ppm) are, on average, also slightly higher in the metasediment-hosted magnetite (Fig. 13A–D). The schlieren type magnetite is richer in Ni compared to metasediment-hosted magnetite, and the magnetite hosted in the Olserum-Djupedal granite exhibits the lowest Ni concentrations. The Sn content (1–15 ppm) is comparatively high in magnetite from the Olserum-Djupedal district relative to magnetite from the other localities studied, whereas the Cr concentration is rather low (1–85 ppm). In the Olserum area, the contents of Al, Ga and Mn increase slightly in metasediment-hosted magnetite closer to the granite contact.

Magnetite from Klockartorpet displays the highest V and Cr concentrations (Cr reaches up to 1 wt%) and low concentrations of Ni, Mn and Ga. Similar to biotite from Gränsö, magnetite from this locality is distinct from magnetite in the Olserum-Djupedal district, and has higher Ni and Cr, and lower Ga and Al concentrations.

In the (Al + Mn) versus (V + Ti) discrimination diagram developed for magnetite from a suite of magmatic and hydrothermal ore deposits (Dupuis and Beaudoin 2011; Nadoll et al., 2014), magnetite from the metasediment-hosted REE ores in the Olserum-Djupedal district plots within the field of high-temperature magmatic-hydrothermal deposits (the IOCG and porphyry-type deposit fields; Fig. 14A). In a plot of Ti versus Ni/Cr suggested by Dare et al. (2014) as a potential tool for discriminating magmatic and hydrothermal magnetite, magnetite from the metasediment- and granite-hosted REE-bearing veins, as well as the magnetite ores in the granite (schlieren), in the Olserum-Djupedal district falls within the hydrothermal field. By contrast, magnetite from the Olserum-Djupedal granite straddles the boundary between the magmatic and hydrothermal fields (Fig. 14B). Magnetite from Klockartorpet, and magnetite from the migmatite at Berg plots well within the field of magmatic magnetite.

4.3.3. Amphibole

Ore-associated amphibole in the Olserum-Djupedal district belongs to the Mg-Fe-Mn subgroup (Hawthorne et al., 2012). Amphibole from Olserum has higher Al (12.6–18.2 wt% Al_2O_3 compared to 1.6–6.5 wt% Al_2O_3) and lower Mg (10.7–12.7 wt% MgO compared to 14.8–16.6 wt% MgO) concentrations than at Djupedal. This classifies the amphibole from the Olserum area as gedrite, and that from Djupedal as anthophyllite (Fig. 15). The Fe contents are similar for both types, and are in the range of 23.0–25.7 wt% FeO in Olserum and 22.8–24.7 wt% FeO in Djupedal. Titanium rarely reaches 0.5 wt% TiO_2 in gedrite in Olserum, and is mostly below the limit of detection (< 0.1 wt% Ti) in Djupedal. Both amphibole types have similar Mn and Ca concentrations, in the

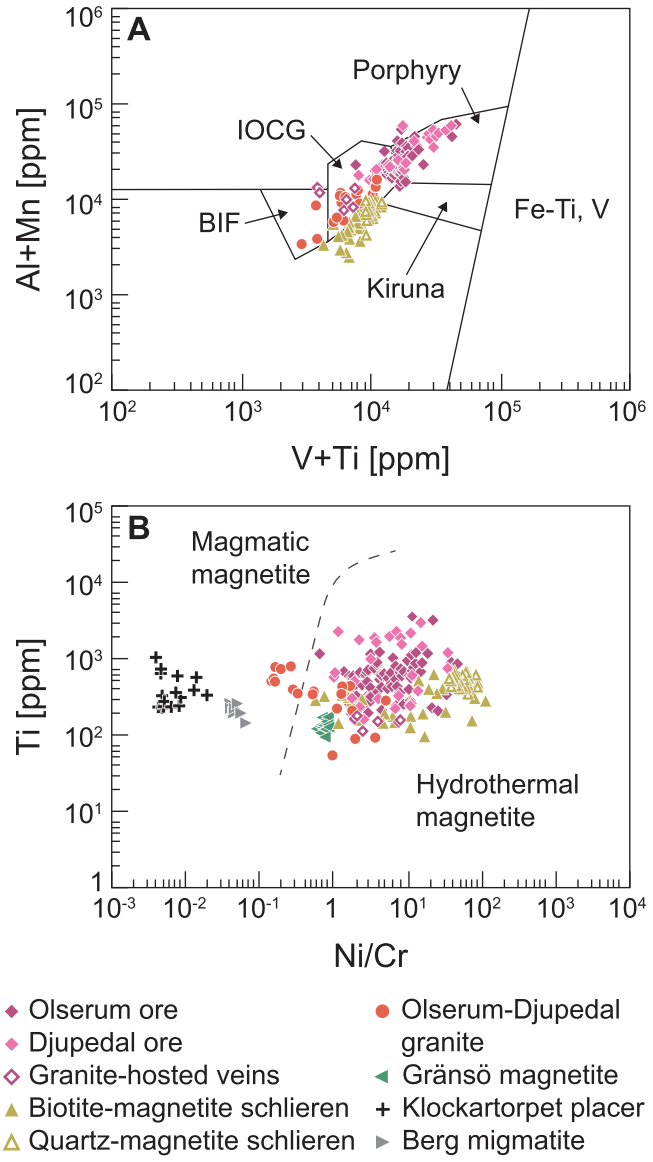

Fig. 14. (A) Composition of magnetite from the Olserum-Djupedal district in the (Al + Mn) against (V + Ti) discrimination diagram of Dupuis and Beaudoin (2011) as modified from Nadoll et al. (2014). (B) Composition of magnetite from the Västervik region in the Ti against Ni/Cr discrimination diagram of Dare et al. (2014).

range of 0.1–0.35 wt% MnO and 0.15–0.5 wt% CaO. Ore-associated gedrite in Olserum has an elevated Na content, which is in the range of 1.7 to 2.3 wt% Na_2O (equivalent to 0.5–0.7 apfu), comparable to the Na enrichment observed for ore-associated biotite. Anthophyllite from Djupedal exhibits overall lower Na concentrations, from 0.1 to 0.7 wt% Na_2O (< 0.2 apfu).

Amphibole locally associated with cordierite often occurs together with an Al-silicate (most likely andalusite) in the REE ore zones and in the host rock at Bersummen. This amphibole type also classifies chemically as gedrite and exhibits a composition similar to the ore-associated gedrite (Fig. 15). No quantitative data for amphibole associated with the breakdown of cordierite (Fig. 10E) in Djupedal were obtained, but EDS analyses indicate a similar composition as the gedrite associated with cordierite.

All analysed gedrite and anthophyllite is OH-dominant, with maximum concentrations of F at 1.0 wt% and of Cl at 0.1 wt%.

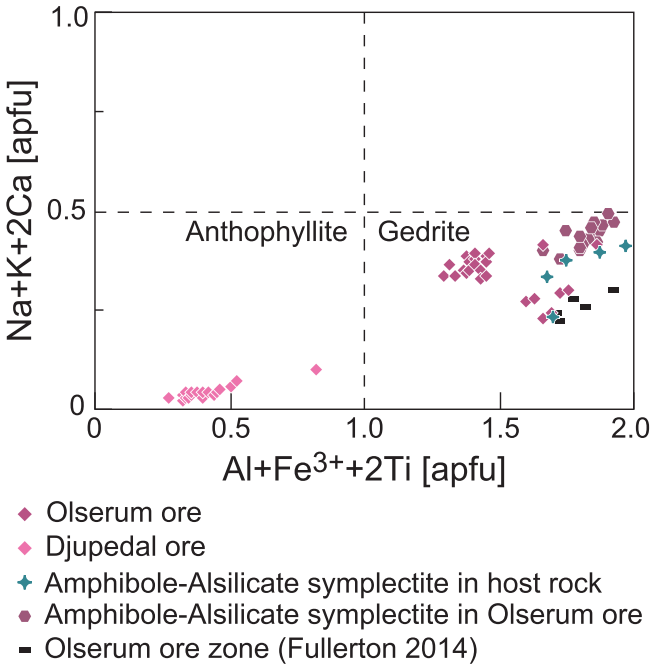

Fig. 15. Plot illustrating the major element chemistry of amphibole from the Olserum-Djupedal REE mineralisation.

Anthophyllite from Djupedal is lower in both F and Cl. The F and Cl data for gedrite co-existing with biotite in the Olserum area show that both elements strongly partition into biotite.

4.3.4. Tourmaline

Tourmaline mainly occurs in the REE ore assemblages in Djupedal within the groundmass surrounding primary xenotime-(Y) and monazite-(Ce) (Fig. 10B and C), and rarely as tourmaline-quartz symplectites. Tourmaline is also present in the Olserum-Djupedal granite and within pegmatites associated with this granite. The ore-associated tourmaline belongs to the alkali- and calcic-groups of tourmalines (Fig. 16A). The symplectitic tourmaline mostly plots in the field of the alkali-group, whereas tourmaline from the groundmass mainly plots into field of the calcic-group. Tourmaline from the granite and pegmatites in the Olserum-Djupedal district plots in the field of the alkali-group. The Ca concentration in the ore-associated tourmaline from the vein groundmass is mainly in the range of 2.3 to 3.7 wt% CaO. The symplectitic tourmaline has low Ca concentration, ranging from 1.0 to 1.9 wt% CaO, whereas tourmaline from the granite and the pegmatites has an even lower Ca concentration, between 0.3 and 1.2 wt% CaO. Conversely, tourmaline from the granite and the pegmatites in the Olserum-Djupedal district is more Na-rich with 1.8 to 2.5 wt% Na_2O. For ore-associated tourmaline, Na is mainly in the range of 0.7 to 1.3 wt% Na_2O.

In a plot of Ca/(Ca + Na) versus Mg/(Mg + Fe), the ore-associated tourmaline within the vein groundmass classifies as uvite but extends slightly towards feruvite (Fig. 16B). The symplectitic tourmaline has a composition ranging from dravite-schorl to uvite, but also straddles the boundary to feruvite. The data also show that Al and Fe increase, and Si and Mg decrease in the ore-associated tourmaline, going from uvite-feruvite towards dravite-schorl. Tourmaline from the granite and the pegmatites in the Olserum-Djupedal district mainly classifies as schorl, while the granite-hosted tourmaline trends towards more dravitic compositions. In terms of the W-site occupancy (OH, O_2, F, Cl), most analysed tourmalines are OH-species, but some would classify as F-species (F > 0.5 apfu).

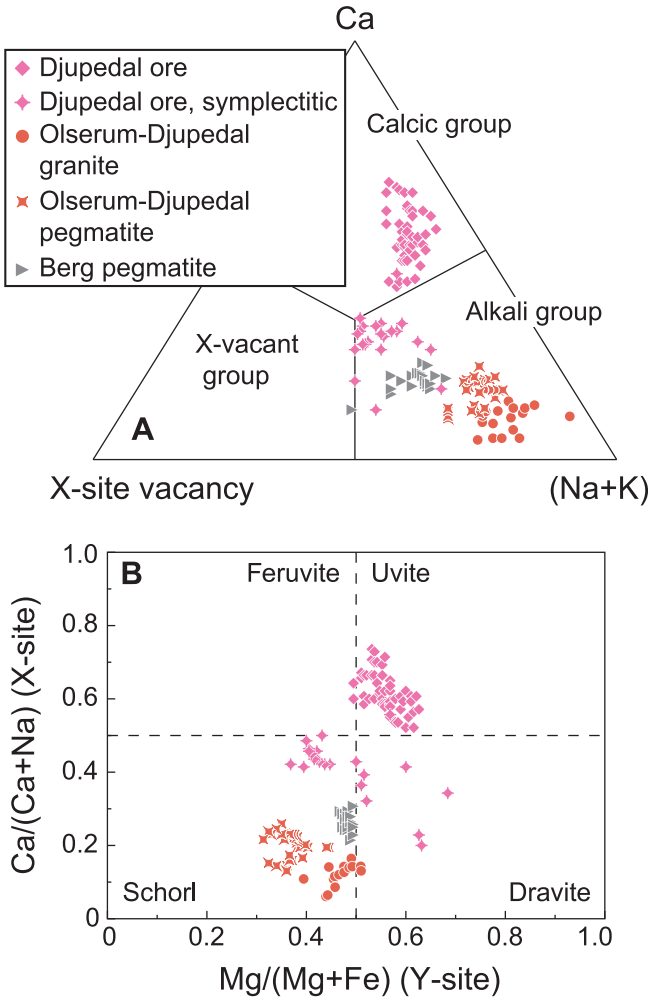

Fig. 16. Diagrams illustrating the major element chemistry of tourmaline from the Olserum-Djupedal REE mineralisation and the migmatitic occurrence in Berg. (A) Classification based on the X-site occupancy (Ca, Na + K and Vacancy). (B) Variation diagram showing the Ca/(Ca + Na) ratio on the X-site as function of the Mg/(Mg + Fe) ratio on the Y-site.

5. Discussion

5.1. Relative timing of REE mineralisation in the Olserum-Djupedal district

The REE ore-associated biotite in the metasedimentary rocks from all three mineralised areas is characterised by high Na and K/Rb and low Ti, and exhibits comparable trace element concentrations to each other. Similarly, the ore-associated magnetite from Olserum and Djupedal has trace element compositions that are very similar to each other, characterised by elevated Al, Mg and V contents. The strikingly similar mineral chemistry of ore-associated biotite and magnetite convincingly demonstrates that the REE mineralisations in all investigated areas are genetically related, and that these REE occurrences form part of a large hydrothermal REE mineralising system, which probably is more extensive than currently known. Although the principal REE-bearing phosphates at Olserum and Djupedal formed during the same primary hydrothermal stage, both localities experienced different post-ore modification histories, as shown by differences in the relationships between the ores and their host rocks (Figs. 6 and 7) as well as their mineralogy (Table 2) and REE mineral alteration features (Andersson et al., 2018).

Several lines of field evidence demonstrate the timing of the initial REE mineralisation stage relative to the alkali feldspar granite emplacement in the Olserum-Djupedal district: (1) the abundant granitic to pegmatitic dykes that cross-cut the REE-bearing veins and vein zones in the Olserum and Bersummen areas (Fig. 6D and E); (2) the granite enclosing REE-mineralised metasedimentary bodies or xenoliths containing cross-cutting granitic dykes in the Djupedal area (Fig. 7D and E); (3) the granite in Djupedal contains inclusions or patches of coarse-grained ore-type biotite with primary REE-bearing fluorapatite (Fig. 7F); (4) migmatised metasediments occur in the Djupedal area, where K-feldspar and quartz melt veins surround fractured primary fluorapatite associated with xenotime-(Y) (Fig. 7B and C). This combined geological evidence suggests that the major REE-phosphate formation occurred early in relation to the magmatic activity and possibly even pre-dates some local anatexis, particularly in the Djupedal area. Despite this, parts of the primary mineralisation must have formed after the crystallisation of the chemically most primitive granite. This is evident from the Olserum area, where biotite-dominated veins carrying monazite-(Ce), xenotime-(Y) and fluorapatite are hosted by the chemically most primitive granite at the contact between the ore-bearing metasedimentary rocks and the major granite body (Fig. 6F and G), and within the transition zone gneisses in the contact zone. Biotite mineral chemistry further demonstrates a distinct connection between metasediment-hosted biotite in REE-bearing veins distal to this contact and biotite in granite-hosted veins. This is demonstrated by, for instance, a systematic increase in Fe and Ti and coupled decrease in Mg and Na in biotite with proximity to the granite-hosted veins (Figs. 11 and 12).

Based on the large body of field and petrographic observations and the mineral-chemical data, we conclude that the unique Olserum-Djupedal style REE mineralisation is closely linked to the emplacement and subsequent evolution of the Olserum-Djupedal granite pluton. This is also corroborated by high crystallisation temperatures of around 600 °C inferred from monazite-xenotime pairs formed during the initial hydrothermal REE stage (Andersson et al., 2018). Unlike in typical felsic magmatic-hydrothermal systems, where associated mineralisations mostly form by fluids exsolved late from a crystallising granite (e.g., Cathelineau et al., 1988; Burnham, 1997, and references therein), the primary REE-phosphates in Olserum-Djupedal formed early in relation to the emplacement and evolution of the granitic pluton. The REE mineralisation is clearly related to the contact aureole of the granite, and the hydrothermal system that formed it was most likely driven by the heat provided by this magma, thus being essentially a high-grade contact metamorphic-hydrothermal mineralising system. The term contact metamorphic-hydrothermal is preferred over magmatic-hydrothermal to emphasise the metamorphic and metasomatic nature of the REE-bearing ore assemblages and textures. Despite this, the dominant fluid source is interpreted to be magmatic.

The REE-phosphates, fluorapatite, (REE,Y,Th,U,Ca)-(Nb,Ta)-oxide (s), biotite, amphibole, magnetite, quartz, ilmenite, and probably minor cordierite, chlorite and muscovite, formed roughly simultaneously in the veins and vein zones during prograde or close to peak metamorphic P-T conditions. However, as shown by the textural relations of mainly biotite, magnetite, amphibole and quartz, these phases were subsequently affected by partial remobilisation and re-equilibration during post-peak to distinctly retrograde processes. This is evident as these gangue, or vein groundmass minerals, both occupy the space around and within the fractured, primary REE minerals and fluorapatite, which were variably fractured and recrystallised during this stage. The textural relations also show that some secondary monazite-(Ce) and xenotime-(Y) clearly formed by later dissolution-reprecipitation processes, as they are anhedral and intergrown with later magnetite and mostly exhibit slightly lower temperatures (down to about 450 °C; Andersson et al., 2018). Allanite-(Ce) and tourmaline in the Djupedal area are not part of the primary assemblages in the veins and vein zones, and both formed later during the evolution of the hydrothermal system. These later-formed REE-bearing phases represent the second stage in the paragenetic evolution (Table 1). The two earliest mineralisation stages (stages A and B) probably reflect a long-lived hydrothermal activity that started prior to, and continued through, the

crystallisation of the chemically most primitive granite. The hydrothermal alteration zones with associated monazite-(Ce), xenotime-(Y) and zircon (Fig. 6H), which have affected the gneissic granite, are further evidence of a hydrothermal overprint of the granite. The absolute age of the REE mineralisation is currently unknown but the relative age is constrained by the U-Pb zircon ages of the granites of the anatectic group in the Västervik region, which are around 1.8 Ga (Kleinhanns et al., 2015). The maximum age of the mineralisation is constrained by the crystallisation age of the chemically most primitive granite cut by minor REE-bearing veins. The minimum age of the mineralisation is given by the migmatisation and the intrusion of the granitic to pegmatitic dykes that cross-cut the REE mineralisation.

The two latest stages of REE mineral formation (Table 1) are probably late- to post-magmatic in relation to the evolving magmatic system. This is because monazite-(Ce) and xenotime-(Y) from the granite-hosted biotite-magnetite schlieren, which formed essentially synchronous with the granite, have been affected by the same type of alteration that overprinted the primary monazite-(Ce) and xenotime-(Y). This post-ore alteration is likely to have occurred during cooling of the granite to at least 1.75 Ga, as indicated by regional disturbances of the Rb-Sr isotopic system in metasedimentary rocks of the Västervik Formation (Kleinhanns et al., 2012), but could potentially even have continued to considerably younger ages.

5.2. Halogen fugacity in the REE-mineralising fluid(s)

Hydrothermal biotite is a major component of the Olserum-Djupedal REE mineralisation, and the halogen composition of biotite can therefore be utilised as an indicator of the halogen fugacity in the hydrothermal fluid(s). This approach has been used for a range of magmatic-hydrothermal systems (e.g., Selby and Nesbitt, 2000; Coulson et al., 2001; Marshall and Oliver, 2006; Monteiro et al., 2008; Afshooni et al., 2013; Iveson et al., 2016; Zhang et al., 2016). The halogen fugacities, expressed as the ratios $\log(f_{H2O}/f_{HF})$, $\log(f_{H2O}/f_{HCl})$ and $\log(f_{HF}/f_{HCl})$, are calculated from the concentrations of F, Cl and OH on the hydroxyl site of biotite using the empirical equations proposed by Munoz (1992). These were, in turn, derived from the revised thermodynamic properties describing the partitioning of F-Cl-OH between biotite and hydrothermal fluids (Zhu and Sverjensky, 1991, 1992). The fugacity ratios are then calculated as follows:

$$\log(f_{H2O}/f_{HF})^{fluid} = (1000/T)\cdot(2.37 + 1.1X_{phl}) + 0.43 - \log(X_F/X_{OH})^{biotite} \quad (1)$$

$$\log(f_{H2O}/f_{HCl})^{fluid} = (1000/T)\cdot(1.15 + 0.55X_{phl}) + 0.68 - \log(X_{Cl}/X_{OH})^{biotite} \quad (2)$$

$$\log(f_{HF}/f_{HCl})^{fluid} = -(1000/T)\cdot(1.22 + 1.65X_{phl}) + 0.25 + \log(X_F/X_{Cl})^{biotite} \quad (3)$$

where

$$X_{phl} = Mg/S_{octahedral\ cations} \quad (4)$$

and T is the equilibrium temperature (in Kelvin), and X_F, X_{Cl} and X_{OH} are the mole fractions of F, Cl and OH in the hydroxyl site of biotite.

To estimate the temperature at which biotite equilibrated with a hydrothermal fluid, we have used the Ti-in-biotite thermometer calibrated for biotite from graphitic, peraluminous metapelites (Henry et al., 2005). This is a justified approach because biotite is paragenetically associated with cordierite and ilmenite in the ore assemblages, and the latter acts as a Ti-saturating mineral, buffering the Ti activity in the system. Moreover, the calculated aluminium saturation index (ASI), i.e., the molar ratio $Al_2O_3/(CaO + Na_2O + K_2O)$, for biotite is greater than 1.4, classifying it as peraluminous in a magmatic environment (Zen, 1988). The absence of graphite in the mineral assemblage, however, may result in a moderate underestimation of the temperatures (Henry et al., 2005). The calculated temperatures for the ore-associated biotite range from below the lower limit of the geothermometer calibration (480 °C) to 575 °C. These are, on average, somewhat lower than the calculated formation temperatures of the primary REE-phosphate minerals, but consistent with the textural position of biotite being locally later-formed, occurring in fractures of the primary, coarse-grained REE minerals. We have therefore used an average temperature of 550 °C for the calculation of halogen fugacities. Biotite from the granite-hosted veins and biotite-magnetite schlieren equilibrated at higher temperatures, around 650 °C, which is also consistent with temperatures calculated from monazite-xenotime geothermometry (Andersson et al., 2018). The regional peak-metamorphic temperature conditions in the Västervik region are supported by the biotite data from the palaeoplacer deposit at Klockartorpet, which yield a temperature range of 675–700 °C.

The ore-associated biotite, including biotite from the granite-hosted veins, yields $\log(f_{H2O}/f_{HCl})$ values of 2.9 to 3.6, $\log(f_{H2O}/f_{HF})$ values of 3.9 to 5.1, and $\log(f_{HF}/f_{HCl})$ values of −2.0 to −0.9 (Fig. 17A and B). Considering that fugacity coefficient terms largely cancel out for these ratios, the $\log(f_{HF}/f_{HCl})$ values imply that the hydrothermal fluid from which the ore-associated biotite formed was enriched in Cl relative to F,

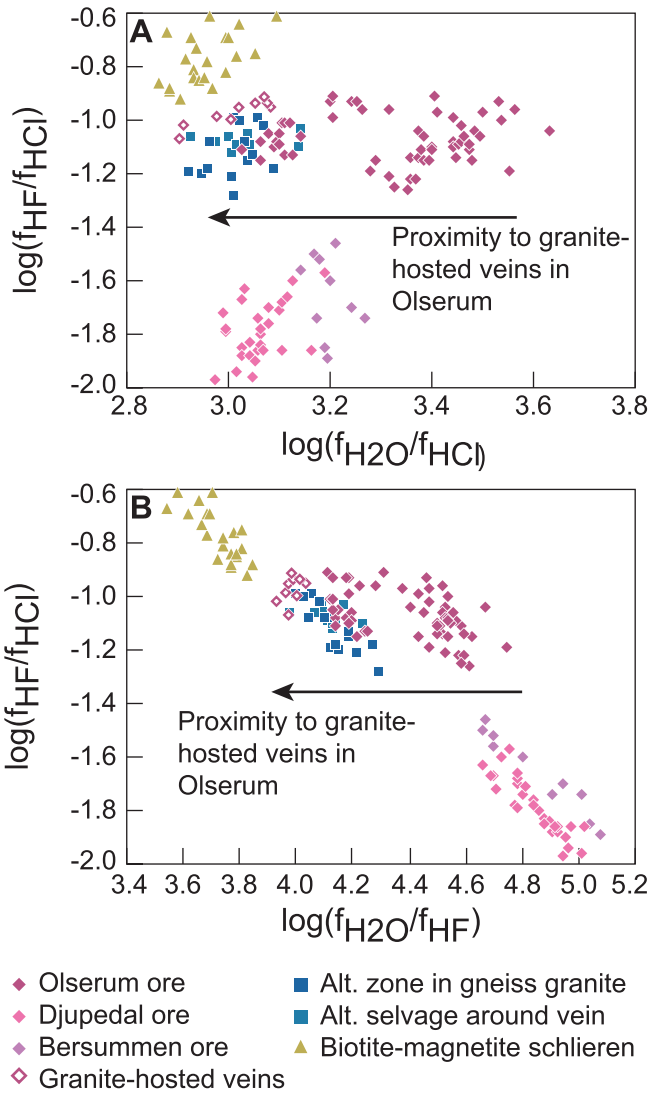

Fig. 17. Diagrams displaying halogen fugacity values in the REE mineralising fluid(s) of the Olserum-Djupedal mineralisation, as calculated from biotite compositions. The fugacity values were calculated from equations in Munoz (1984, 1992). (A) $\log(f_{HF}/f_{HCl})$ against $\log(f_{H2O}/f_{HCl})$ (B) $\log(f_{HF}/f_{HCl})$ against $\log(f_{H2O}/f_{HF})$.

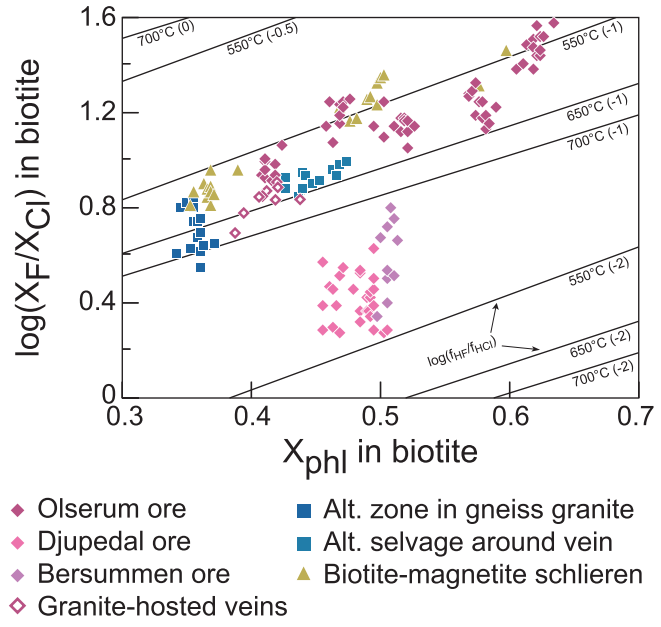

Fig. 18. Diagram illustrating the $\log(X_F/X_{Cl})$ against X_{phl} of biotite. The reference lines show the $\log(f_{HF}/f_{HCl})$ values calculated at different temperatures using the equations from Munoz (1992).

as expected in most hydrothermal fluids. The actual ratios of f_{HF}/f_{HCl} (between 0.01 and 0.12) would, however, suggest elevated F concentrations in the fluids. Moreover, calculated $\log(f_{HF}/f_{HCl})$ values do also show that biotite from the Djupedal and Bersummen areas (log values: −2.0 to −1.5) formed from fluid(s) with almost an order of magnitude lower HF concentration compared to the Olserum area (log values: −1.3 to −0.9), independent of the temperature of the equilibrated fluid(s) (Fig. 18). In a plot showing $\log(X_F/X_{Cl})$ as a function of the mole fraction of phlogopite (X_{phl}), any biotite that equilibrated with a hydrothermal fluid at constant temperature and $\log(f_{HF}/f_{HCl})$ should plot along straight lines (Zhu and Sverjensky, 1991). Indeed, biotite from the REE mineralisation in the Olserum area has a rather constant $\log(f_{HF}/f_{HCl})$ value of about -1 for a temperature of 550–600 °C. This value remains constant, but the temperature increases towards the contact to the granite and within the granite-hosted veins (Fig. 18). This increase in temperature closer to the granite contact is supported by the biotite and monazite-xenotime geothermometry.

In comparison, the $\log(f_{H2O}/f_{HCl})$ values of 2.9–3.6 and $\log(f_{H2O}/f_{HF})$ values of 3.9–5.1 calculated for the REE mineralising hydrothermal system in Olserum-Djupedal, are generally lower than in magmatic-hydrothermal porphyry deposits as calculated from biotite compositions. These typically have $\log(f_{H2O}/f_{HCl})$ values of 3.7–5.5 and $\log(f_{H2O}/f_{HF})$ values of 4.5–6.6 (e.g., Selby and Nesbitt, 2000; Afshooni et al., 2013; Iveson et al., 2016). The calculated $\log(f_{H2O}/f_{HCl})$ values are comparable to those of IOCG deposits such as at the Sossego deposit, Brazil ($\log(f_{H2O}/f_{HCl})$: 2.5–3.0; Monteiro et al., 2008) and deposits from the Mt. Isa Block, Australia ($\log(f_{H2O}/f_{HCl})$: 2.8–3.6; Marshall and Oliver, 2006). This suggests that the Olserum-Djupedal hydrothermal system was dominated by fluids with comparably high HCl and HF fugacities, similar to IOCG systems.

5.3. Origin of the Olserum-Djupedal REE mineralisation

The Olserum-Djupedal REE mineralisation represents an example of an unusual type of REE (± Th, U) deposit dominated by the REE-phosphates monazite-(Ce) and xenotime-(Y), and variably REE-bearing fluorapatite associated with biotite and amphibole. To our knowledge, only very few comparable REE occurrences are known worldwide, for instance the REE mineralisation in the Pinto Gneiss in the Music Valley, California, USA (McKinney et al., 2015) or the REE mineralised monazite-xenotime gneiss in the Hudson Highlands, New York, USA (Aleinikoff et al., 2012). The primary enrichment of REE in the Music Valley deposit was interpreted as magmatic, followed by later metasomatic alteration. The origin of the REE mineralisation in the Hudson Highlands was thought to be caused by metasomatism associated with high-grade metamorphism (> 700 °C) with repeated post-ore remobilisation processes affecting the primary mineralisation.

Two main origins for the U ± REE mineralisations in the Västervik region have been proposed previously: (1) former fluvial heavy mineral enrichments (palaeoplacers), which were partly remobilised during the emplacement of the younger granites (Welin, 1966a,b), or (2) a hydrothermal origin related to regional large-scale Na ± Ca metasomatism (Hoeve, 1974, 1978). The geological observations and geochemical data for the Olserum-Djupedal REE-phosphate mineralisation are clearly inconsistent with a model of remobilised palaeoplacers and instead support a hydrothermal model and a direct genetic link with the younger granites, based on the following key arguments. Firstly, the primary REE-phosphate mineralisation in the Olserum-Djupedal district has a mineralogy that is very different from that of true palaeoplacers. The palaeoplacer deposits are mainly composed of rather fine-grained and mostly anhedral magnetite, zircon, rutile, ilmenite with only minor amounts of monazite, unidentified U-phases, tourmaline and apatite (this study; Gavelin, 1984), and potentially davidite, brannerite and anatase (Gustafsson, 1990). By contrast, the primary REE mineralisation of the Olserum-Djupedal district contains essentially no primary zircon and rutile, but is instead dominated by very coarse-grained monazite-(Ce), xenotime-(Y) and fluorapatite. Importantly, the primary REE-phosphates monazite-(Ce) and xenotime-(Y) are present as euhedral to subhedral crystals with large crystal sizes of typically several cm, and sometimes up to 10 cm. This characteristic occurrence of these dominant primary REE-phosphates cannot be reconciled with a palaeoplacer model. Secondly, the mineral chemistry of both magnetite and biotite clearly discriminates the true palaeoplacer deposits from the hydrothermal REE mineralisation in the Olserum-Djupedal district. Finally, and most importantly, the biotite-dominated REE-phosphate-bearing veins clearly do not represent heavy mineral layers. The veins occur as individual veins (Fig. 6E) or sets of interconnected veins (Fig. 6A) with variable widths that locally pinch out or terminate abruptly. In addition, the vein zones have thicknesses of up to several metres (as observed in outcrops and drill cores in Olserum).

The proposed hydrothermal origin for the U ± REE mineralisations in the Västervik region as well as the connection with regional-scale Na ± Ca metasomatism was based on the presence of characteristic quartz-plagioclase rocks (Hoeve, 1974, 1978). The genetic link between the regional metasomatism and hydrothermal mineralisation was in turn based on geochemical data for least altered rocks, altered equivalents and the mineralisations themselves, combined with mass balance calculations. The protoliths of the quartz-plagioclase rocks were interpreted to be metasedimentary rocks from the Västervik Formation and older Loftahammar-type granitoids.

A metasomatic quartz-plagioclase rock is present in the Djupedal area and its textural relations show that K-feldspar has been extensively replaced by plagioclase (albite to oligoclase in composition) and that the accessory minerals are replaced by various Ca-bearing minerals (Fig. 9B and D). This style of alteration indicates that similar Na ± Ca metasomatism (or sodic-calcic alteration) to that described by Hoeve (1974, 1978) affected the Olserum-Djupedal district. Similarly altered perthitic K-feldspar and plagioclase in the Olserum-Djupedal granite (Fig. 9F) suggest that the Na ± Ca metasomatic event operated after the entire granite had crystallised during subsolidus conditions, and thus post-dated the primary hydrothermal REE stage. The transitional contact between the quartz-plagioclase rock and the porphyritic granitoid rocks belonging to the quartz monzonite (QM) suite indicates that the metasomatic alteration also affected these slightly older rocks.

The unusually high Na contents in the ore-associated hydrothermal

biotite (up to 1 wt% Na_2O) and gedrite (up to 2.3 wt% Na_2O), as well as in the fluorapatite (200–1200 ppm; Andersson et al., 2017), indicate that the fluid responsible for the primary hydrothermal REE stage was rich in Na. This high Na content was probably not attained via rock buffering with the surrounding host rocks because both the granite and the metasedimentary rocks do not exhibit exceptionally high Na concentrations. Rather, the REE-mineralising fluid likely represented a high-salinity fluid expelled from the granite. Because of the abundance of biotite precipitated from this fluid, the high-temperature fluid probably had a high K/Na ratio, either obtained by direct expulsion of relatively K-rich fluids or from initial fluid-rock interactions with the K-feldspar-rich Olserum-Djupedal granite, and the fluid also had a relatively high Na content and a low Ca/Na ratio. Importantly, the low Ca concentration promoted the available phosphate in the fluid to mostly precipitate as abundant REE-phosphates instead of only fluorapatite. In the Olserum area, biotite records an increase in the Na content from the REE-bearing veins hosted in the granite towards metasediment-hosted veins distal to the granite. This may suggest that the fluid became relatively enriched in Na and depleted in K during the evolution of the hydrothermal system. During subsequent cooling, the fluid locally evolved to Ca-rich compositions as indicated by the Ca-rich minerals allanite-(Ce) and particularly tourmaline (uvite to feruvite; Fig. 16) in the Djupedal area. Uvitic tourmaline is uncommon in typical felsic magmatic and metamorphic settings and requires a Ca-rich fluid or the interaction of the fluid with Ca-rich host rocks to form (Henry and Dutrow, 1996; Slack, 1996; London, 1999; Van Hinsberg et al., 2011). The proximity of this area to the older QM (Fig. 2), which generally is richer in Ca, may partly explain the greater calcic component in the fluid, in addition to the predicted increase of the Ca content in the fluid that occurs via granite-fluid interactions during cooling in magmatic-hydrothermal systems (Dolejš and Wagner, 2008). Subsequent alteration of primary monazite-(Ce) in the Djupedal area and partial alteration of monazite-(Ce) in the granite-hosted schlieren, which requires Ca-rich fluids, was probably related to the Na ± Ca metasomatism identified in the quartz-plagioclase rock and in the Olserum-Djupedal granite. The hydrothermal REE mineralisation thus likely formed in association with initial high-temperature (about 600 °C) K-Na metasomatism (potassic-sodic alteration) manifested by abundant Na-rich biotite and later evolved to low to medium-high temperature (200–500 °C) Na-Ca metasomatism (sodic-calcic alteration) causing distinct differences in mineralogy and alteration features between both areas.

Even though Hoeve (1974, 1978) never described or recognised any K-rich metasomatism in his study area (mainly south of Loftahammar; Fig. 1), it is likely that the metasomatic alteration described by him and the one in the Olserum-Djupedal area are related, potentially representing part of a larger regional alteration system. Hoeve (1974) suggested that the Na ± Ca metasomatism and the associated U ± REE mineralisations to mainly be slightly older than the younger granites, which contradicts the observation that feldspar from the Olserum-Djupedal granite exhibits similar alteration features as the quartz-plagioclase rocks. However, Hoeve (1974) still considered the generation of the granites and the Na ± Ca metasomatism to be coeval but operating at different crustal depths. A clear connection between the area south of Loftahammar and the Olserum-Djupedal district is that the younger granites in both areas share many features. The younger granites in the Loftahammar area commonly show associated migmatitic aureoles, pegmatites within and outside the intrusions, and they exhibit border zones enriched in allanite, monazite, apatite, titanite, magnetite, plagioclase and biotite (Hoeve, 1974). The mineral assemblage of the associated fracture-hosted U ± REE mineralisations in the area south of Loftahammar is, however, quite unlike that of the Olserum-Djupedal REE mineralisation. These U ± REE mineralisations typically contain primary rutile, ilmenite, davidite [(Ce,La)(Y,U,Fe)$(Ti,Fe)_{20}(O,OH)_{38}$], allanite and thorite and subordinate zircon (potentially also xenotime), apatite, monazite, scheelite and biotite, and secondary pyrite, hematite, titanite and scapolite. Biotite is invariably present in the mineralised fractures in smaller amounts, filling microfractures and enclosing aggregates of ore minerals. At some localities, however, biotite predominantly forms veins and patches up to one metre wide and several tens of metres long, occasionally with abundant apatite (island of Norra Malmö) and monazite (island of Björkö) (Hoeve, 1974). These latter two occurrences resemble the vein-hosted REE mineralisation in the Olserum-Djupedal district and may be a manifestation of the high-temperature K-Na metasomatism. However, the other REE occurrences richer in Ti-bearing minerals may represent another style of mineralisation formed from the leached elements by the later Na ± Ca metasomatism as suggested by Hoeve (1974), which is potentially not exposed or not yet discovered in the Olserum-Djupedal district.

This potentially regional-scale metasomatic system was active concomitantly with heat production from the anatectic granites and associated metamorphism around 1.8 Ga. This magmatic-metamorphic event is also broadly coeval with the development of crustal-scale shear zones within the NW-SE-oriented Loftahammar-Linköping Deformation Zone (LLDZ; Fig. 1) at 1800–1780 Ma (Beunk and Page, 2001). Whether these shear zones may have served as fluid pathways, aiding regional-scale metasomatism and the formation of U ± REE mineralisations, remains speculative. Several other REE occurrences and old magnetite mines in the Västervik region (e.g., Ramstad south of Olserum-Djupedal, Borsjö north of Olserum-Djupedal, and Björknäs southwest of Olserum-Djupedal; Geijer and Magnusson, 1944) lack modern studies, but seem to share some features with the REE mineralisation in the Olserum-Djupedal district, and may be related to the same regional hydrothermal system.

5.4. The source of REE and P

The ultimate source of the REE and of P for the mineralisation in the Olserum-Djupedal district remains one of the key questions. The metasedimentary rocks may have been pre-enriched in REE and P through sedimentary processes and subsequently completely overprinted by the mineralising event and granite intrusions. However, it is difficult to convincingly demonstrate such a process with the data at hand. This model would also face a fundamental problem when considering mass balance. The known palaeoplacer deposits in the Västervik Formation (e.g., Klockartorpet) have quite low concentrations of REE and P (as well as of Th and U), but they are particularly rich in Zr (and Hf). This contrasts with the abundance of REE and P (and Th and U) and the low concentrations of Zr (and Hf) in the REE mineralisation in the Olserum-Djupedal district. Moreover, the palaeoplacers are mostly present as sparsely occurring, thin layers (typically < 2 cm in thickness), which are intercalated in the quartzites of the Västervik Formation. If the palaeoplacers were the source of the REE and of P, this would require fluid flow models where hydrothermal fluids released from the granites first interact with a very large body of rock containing small palaeoplacer beds and selectively mobilise the REE and P compared to the remaining element suite found in the palaeoplacers. This fluid would then need to be drained from a large volume of rock and focused into a single well-defined structural zone that hosts the REE mineralisations. Such a model cannot be reconciled with the fluid flow regime that would develop in response to the temperature and pressure gradients produced by a large granitic pluton emplaced into relatively cooler wall rocks, where fluids are expelled from the intrusion and infiltrate the surrounding host rocks. (Hansen, 1995; Ingebritsen and Appold, 2012).

The most plausible model for the REE mineralisation is that REE and P were derived from the Olserum-Djupedal granite by fluid interaction with the crystallising granitic magma. The granite is, however, not particularly enriched in REE (ΣREE + Y is about 300 ppm) nor P (0.04–0.07 wt% P_2O_5) compared to for instance other suites in the Västervik region (Nolte et al., 2011). The granite is locally enriched in REE minerals, containing accessory monazite-(Ce), xenotime-(Y) and

allanite-(Ce), mainly concentrated in the schlieren but also as individual crystals and aggregates in the granite groundmass. If the primary REE mineralisation essentially formed by a fluid exsolved early from the crystallising granitic magma, this fluid may have partitioned most of the REE and P, leaving the remaining granitic magma relatively depleted in these elements, explaining the relatively lower REE content in the granite. One other potential indicator of a magmatic source is the B required to form tourmaline in the ore assemblages in the Djupedal area, which likely formed by B-rich fluids derived from the granite because tourmaline is a primary component in the granite and frequently occurs within the late pegmatitic to granitic dykes. The occurrences of tourmaline-rich rocks formed by such fluids are commonly developed within contact metasomatic aureoles near granitic intrusions (Slack, 1996, and references therein).

The granite-derived fluid may also have locally interacted with the adjacent QM suite, which generally contains higher concentrations of REE and P (ΣREE + Y: 200–500 ppm; P_2O_5: 0.2–0.5 wt%; Nolte et al., 2011) to attain higher contents of REE and P. However, the ultimate source of REE and P must be the local granite because of the strong spatial and temporal relation of the REE mineralisation to this granite and the physically unrealistic fluid flow model and selective leaching that would be necessary for any genetic model involving palaeoplacers as a source for REE and P. The REE mineralisation essentially formed by high-temperature fluids derived from the granite and expelled early in its evolution, and mainly developed within the contact aureole of the granite. The mineralisation thus represents a contact metamorphic-hydrothermal system rather than a typical magmatic-hydrothermal system.

6. Conclusions

The REE mineralisation in the Olserum-Djupedal district provide fundamental insight into the key processes leading to the formation of high-temperature REE mineralisation. The REE-phosphate mineralisation at Olserum-Djupedal represent an unusual vein-type mineralisation with abundant monazite-(Ce), xenotime-(Y) and variably REE-bearing fluorapatite. The large body of geological and petrographic observations and mineral chemical data are in strong disagreement with a model where the REE mineralisation represents a modified palaeoplacer deposit, and are best reconciled with a hydrothermal origin closely associated with alkali feldspar granite emplacement at around 1.8 Ga.

The REE-phosphate mineralisation developed primarily in metasedimentary rocks in the contact aureole of the granite but also within the chemically most primitive and earliest-formed granite present at the contact between the metasedimentary rocks and the granitic pluton. Primary REE mineralisation formed early in the magmatic evolution, from granite-derived fluids and the REE-minerals formed at this stage were variably altered during subsequent cooling and evolution of the magmatic and hydrothermal system. The crystallisation age of the chemically most primitive granite, around 1.8 Ga, defines the maximum age of the primary mineralisation. The migmatisation and the intrusion of granitic to pegmatitic dykes cross-cutting the REE ore delimit the minimum age, which should be slightly younger than 1.8 Ga. Subsequent stages of alteration were likely active to at least 1.75 Ga, and potentially even younger.

The halogen chemistry of ore-associated biotite indicates rather high concentrations of HCl but, importantly, also high HF for the original REE mineralising fluid. The $\log(f_{HF}/f_{HCl})$ values calculated from biotite in the Olserum area suggest a rather constant value of about −1 at temperatures from about 650 °C to 550–600 °C, during the progressive evolution of the primary REE hydrothermal system away from the granite contact. In the Djupedal and Bersummen areas, the fluid that formed the REE mineralisation was characterised by higher HCl concentrations compared to Olserum.

The Olserum-Djupedal REE mineralisation likely formed during initial high-temperature K-Na metasomatism, which locally evolved into Na-Ca metasomatism that variably altered the primary ore assemblages and host rocks during late- to post-magmatic conditions. The Na-Ca metasomatic alteration stage is potentially linked to a previously recognised regional Na ± Ca metasomatism and associated fracture-hosted U ± REE mineralisation event that was active contemporaneously with anatectic granite magmatism around 1.8 Ga. This strongly indicates the high potential for new REE deposit discoveries and highlights the usefulness of re-investigating previously known deposits in this still rather poorly studied area.

Acknowledgments

This study was supported by a GeoDoc Graduate Programme (Graduate School, Faculty of Sciences, University of Helsinki) grant to Stefan S. Andersson and complementary funding from the Academy of Finland (Project No. 280458) to Thomas Wagner. Erik Jonsson acknowledges support from the Swedish Research Council (Vetenskapsrådet) to Uppsala University, and from the Geological Survey of Sweden (SGU). We thank Tasman Metals and Leading Edge Materials for support during field work and for granting access to proprietary information. The staff of the SGU national drillcore archive in Malå is thanked for their kind support during logging and sampling of drill cores. We thank Helena Korkka for the preparation of thin and thick sections, Radoslaw Michallik for assistance with electron-probe microanalysis, and Dina Schultze for the help with cathodoluminescence imaging. We also would like to thank two anonymous Ore Geology Reviews reviewers for their constructive comments on this manuscript.

References

Afshooni, S.Z., Mirnejad, H., Esmaeily, D., Asadi Haroni, H., 2013. Mineral chemistry of hydrothermal biotite from the Kahang porphyry copper deposit (NE Isfahan), Central Province of Iran. Ore Geol. Rev. 54, 214–232.

Aleinikoff, J.N., Grauch, R.I., Mazdab, F.K., Kwak, L., Fanning, C.M., Kamo, S.L., 2012. Origin of an unusual monazite-xenotime gneiss, Hudson Highlands, New York: Shrimp U-Pb geochronology and trace element geochemistry. Am. J. Sci. 312, 723–765.

Andersen, T., Andersson, U.B., Graham, S., Åberg, G., Simonsen, S.L., 2009. Granitic magmatism by melting of juvenile continental crust: new constraints on the source of Palaeoproterozoic granitoids in Fennoscandia from Hf isotopes in zircon. J. Geol. Soc. London 166, 233–247.

Andersson, S.S., Wagner, T., Jonsson, E., 2017. Fluorapatite as a fluid tracer in the hydrothermal Olserum-Djupedal REE mineralisation, SE Sweden. Abstract from Goldschmidt 2017, Paris, France.

Andersson, S.S., Wagner, T., Jonsson, E., Michallik, R.M., 2018. Mineralogy, paragenesis and mineral chemistry of REEs in the Olserum-Djupedal REE-phosphate mineralization, SE Sweden. Am. Mineral. 103, 125–142.

Barton, M.D., Ilchik, R.P., Marikos, M.A., 1991. Metasomatism. Rev. Mineral. 26, 321–350.

Bergström, U., Juhojuntti, N., Kero, L., Lundqvist, L., Stephens, M.B., Sukotjo, S., Wik, N. G., Wikman, H., 2002. Projekt Småland, regionalt berg. In: Delin, H. (Ed.), Regional berggrundsgeologisk undersökning. Sammanfattning av pågående undersökningar 2001. Sveriges Geologiska Undersökning Rapporter och Meddelanden 110, pp. 65-83.

Beunk, F.F., Page, L.M., 2001. Structural evolution of the accretional continental margin of the Paleoproterozoic Svecofennian orogen in southern Sweden. Tectonophysics 339, 67–92.

Billström, K., Broman, C., Söderhielm, J., 2004. The Solstad Cu ore - an Fe oxide-Cu-Au type deposit in SE Sweden. GFF 126, 147–148.

Burnham, C.W., 1997. Magmas and hydrothermal fluids. In: Barnes, H.L. (Ed.), Geochemistry of Hydrothermal Ore Deposits, 3rd ed. John Wiley and Sons, New York, pp. 63–123.

Cathelineau, M., Marignac, C., Dubessy, J., Poty, B., Weisbrod, A., Ramboz, C., Leroy, J., 1988. Fluids in granitic environment. Rendiconti Della Societá Italiana di Mineralogia e Petrologia 43, 263–274.

Chakhmouradian, A.R., Zaitsev, A.N., 2012. Rare earth mineralization in igneous rocks: Sources and processes. Elements 8, 347–353.

Coulson, I.M., Dipple, G.M., Raudsepp, M., 2001. Evolution of HF and HCl activity in magmatic volatiles of the gold-mineralized Emerald Lake pluton, Yukon Territory, Canada. Miner. Deposita 36, 594–606.

Cox, S.F., 2005. Coupling between deformation, fluid pressures, and fluid flow in ore-producing hydrothermal systems at depth in the crust. Econ. Geol. 100th Anniversary Volume, 39–76.

Dare, S.A.S., Barnes, S.J., Beaudoin, G., Méric, J., Boutroy, E., Potvin-Doucet, C., 2014. Trace elements in magnetite as petrogenetic indicator. Miner. Deposita 49, 745–763.

Djenchuraeva, R.D., Borisov, F.I., Pak, N.T., Malyukova, N.N., 2008. Metallogeny and geodynamics of the Aktiuz-Boordu mining district, northern Tien Shan, Kyrgyzstan. J. Asian. Earth. Sci. 32, 280–299.
Dolejš, D., Wagner, T., 2008. Thermodynamic modeling of non-ideal mineral-fluid equilibria in the system Si–Al–Fe–Mg–Ca–Na–K–H–O–Cl at elevated temperatures and pressures: Implications for hydrothermal mass transfer in granitic rocks. Geochim. Cosmochim. Acta 72, 526–553.
Dupuis, C., Beaudoin, G., 2011. Discriminant diagrams for iron oxide trace element fingerprinting of mineral deposit types. Miner. Deposita 46, 319–335.
Elbers, F.J., 1971. Evolution of the Svecofennian orogeny in the northeastern part of the Västervik area, southeastern Sweden, with special reference to deformation, metamorphism and magmatism. Ph.D. thesis. Vrije University, Amsterdam, pp. 56 pp.
Elliott, H.A.L., Wall, F., Chakhmouradian, A.R., Siegfried, P.R., Dahlgren, S., Weatherley, S., Finch, A.A., Marks, M.A.W., Dowman, E., Deady, E., 2018. Fenites associated with carbonatite complexes: a review. Ore Geol. Rev. 93, 38–59.
Frietsch, R., Perdahl, J.A., 1995. Rare earth elements in apatite and magnetite in Kiruna-type iron ores and some other iron ore types. Ore Geol. Rev. 9, 489–510.
Frost, B.R., Barnes, C.G., Collins, W.J., Arculus, R.J., Ellis, D.J., Frost, C.D., 2001. A geochemical classification for granitic rocks. J. Petrol. 42, 2003–2048.
Fullerton, W., 2014. REE mineralisation and metasomatic alteration in the Olserum metasediments. M.Sc. thesis. Lund University, pp. 86 pp.
Gaál, G., Gorbatschev, R., 1987. An outline of the Precambrian evolution of the Baltic shield. Precambrian Res. 35, 15–52.
Gavelin, S., 1984. The Västervik area in south-eastern Sweden. Studies in Proterozoic sedimentation, high-grade metamorphism and granitization. Sveriges Geologiska Undersökning Ba 32, 172 pp.
Geijer, P., Magnusson, N.H., 1944. De mellansvenska järnmalmernas geologi. Sveriges Geologiska Undersökning Ca 35, 654 pp.
Goodenough, K.M., Schilling, J., Jonsson, E., Kalvig, P., Charles, N., Tuduri, J., Deady, E.A., Sadeghi, M., Schiellerup, H., Müller, A., Bertrand, G., Arvanitidis, N., Eliopolous, D.G., Shaw, R.A., Thrane, K., Keulen, N., 2016. Europe's rare earth element resource potential: an overview of metallogenetic provinces and their geodynamic setting. Ore Geol. Rev. 72, 838–856.
Gorbatschev, R., 2004. The Transscandinavian Igneous Belt – Introduction and background. Geol. S. Finl. 37, 9–15.
Guillong, M., Meier, D.L., Allan, M.M., Heinrich, C.A., Yardley, B.W.D., 2008. SILLS: a MATLAB-based program for the reduction of laser ablation ICP-MS data of homogeneous materials and inclusions. Mineralogical Association of Canada Short Course Volumes 40, 328–333.
Gustafsson, B., 1990. Sällsynta jordartsmetaller i Sverige. Sveriges Geologiska AB, PRAP 90024 (NSG 90049). 1–29.
Gustafsson, B., 1992. Sällsynta jordartsmetaller: regional fältkontroll 1991 av arkivuppslag. Sveriges Geologiska AB, PRAP 91047, 1–22.
Hansen, R.B., 1995. The hydrodynamics of contact metamorphism. Geol. Soc. Am. Bull. 107, 595–611.
Hawthorne, F.C., Oberti, R., Harlow, G.E., Maresch, W.V., Martin, R.F., Schumacher, J.C., Welch, M.D., 2012. Nomenclature of the amphibole supergroup. Am. Mineral. 97, 2031–2048.
Hedenquist, J.W., Lowenstern, J.B., 1994. The role of magmas in the formation of hydrothermal ore deposits. Nature 370, 519–527.
Heinrich, C.A., Candela, P.A., 2013. Fluids and ore formation in the Earth's crust. Treatise Geochem. 13, 1–28.
Henry, D.J., Dutrow, B.L., 1996. Metamorphic tourmaline and its petrological applications. Rev. Mineral. 33, 503–557.
Henry, D.J., Guidotti, C.V., Thomson, J.A., 2005. The Ti-saturation surface for low-to-medium pressure metapelitic biotites: Implications for geothermometry and Ti-substitution mechanisms. Am. Mineral. 90, 316–328.
Hoeve, J., 1974. Soda metasomatism and radio-active mineralisation in the Västervik area, southeastern Sweden. Ph.D. thesis. Vrije University, Amsterdam, pp. 191 pp.
Hoeve, J., 1978. Composition and volume changes accompanying soda metasomatic alterations, Västervik area, SE Sweden. Geol. Rundsch. 67, 920–942.
Holtstam, D., Andersson, U.B., 2007. The REE minerals of the Bastnäs-type deposits, south-central Sweden. Can. Mineral. 45, 1073–1114.
Holtstam, D., Andersson, U.B., Broman, C., Mansfeld, J., 2014. Origin of REE mineralization in the Bastnäs-type Fe-REE-(Cu-Mo-Bi-Au) deposits, Bergslagen, Sweden. Miner. Deposita 49, 933–966.
Ingebritsen, S.E., Appold, M.S., 2012. The physical hydrogeology of ore deposits. Econ. Geol. 107, 559–584.
Iveson, A.A., Webster, J.D., Rowe, M.C., Neill, O.K., 2016. Magmatic-hydrothermal fluids and volatile metals in the Spirit Lake pluton and Margaret Cu-Mo porphyry system, SW Washington, USA. Contrib. Mineral. Petr. 171, 1–32.
Jonsson, E., Högdahl, K., Sahlström, F., Nysten, P., Sadeghi, M., 2014. The Palaeoproterozoic skarn-hosted REE mineralisations of Bastnäs-type: overview and mineralogical-geological character. In: Balomenos, E., Panias, D., Paspaliaris, I. (Eds.), ERES2014: 1st European Rare Earth Resource Conference, Milos, Proceedings, pp. 382–389.
Jonsson, E., Harlov, D.E., Majka, J., Högdahl, K., Person-Nilsson, K., 2016. Fluorapatite-monazite-allanite relations in the Grängesberg apatite-iron oxide ore district, Bergslagen, Sweden. Am. Mineral. 101, 1769–1782.
Kesler, S.E., 2005. Ore-forming fluids. Elements 1, 13–18.
Kleinhanns, I.C., Fischer-Goedde, M., Hansen, B.T., 2012. Sr–Nd isotope and geochemical characterisation of the Paleoproterozoic Västervik formation (Baltic Shield, SE Sweden): a southerly exposure of Svecofennian metasiliciclastic sediments. Int. J. Earth Sci. 101, 39–55.
Kleinhanns, I.C., Whitehouse, M.J., Nolte, N., Baero, W., Wilsky, F., Hansen, B.T., Schoenberg, R., 2015. Mode and timing of granitoid magmatism in the Västervik area (SE Sweden, Baltic Shield): Sr-Nd isotope and SIMS U-Pb age constraints. Lithos 212–215, 321–337.
Korja, A., Lahtinen, R., Nironen, M., 2006. The Svecofennian orogen: a collapse of microcontinents and island arcs. Geo. Soc. Mem. 32, 561–578.
Kresten, P., 1971. Metamorphism and migmatization in the Västervik area, SE Sweden. Geol. Fören. Stock. Förh. 93, 743–764.
Kresten, P., 1986. The granites of the Västervik area, south-eastern Sweden. Sveriges Geologiska Undersökning C 814, 35 pp.
Kresten, P., Morogan, V., 1986. Fenitization at the Fen complex, southern Norway. Lithos 19, 27–42.
Linthout, K., 2007. Tripartite division of the system 2 REEPO4 – CaTh(PO4)2–2 ThSiO4, discrediation of brabantite, and recognition of cheralite as the name for members dominated by CaTh(PO4)2. Can. Mineral. 45, 243–248.
Lira, R., Ripley, E.M., 1990. Fluid inclusion studies of the Rodeo de Los Molles REE and Th deposit, Las Chacras Batholith, Central Argentina. Geochim. Cosmochim. Acta 54, 663–671.
Locock, A.J., 2014. An Excel spreadsheet to classify chemical analyses of amphiboles following IMA 2012 recommendations. Comput. Geosci. 62, 1–11.
Löfvendahl, R., Åkerblom, G., 1976. Uranprospektering i Västerviksområdet. Rapport över av SGU utförda prospekteringsarbeten åren 1970–1974. Sveriges Geologiska Undersökning BRAP 87003, 1–146.
London, D., 1999. Stability of tourmaline in peraluminous granite systems: the boron cycle from anatexis to hydrothermal aureoles. Eur. J. Mineral. 11, 253–262.
Mansfeld, J., Beunk, F.F., Barling, J., 2005. 1.83-1.82 Ga formation of a juvenile volcanic arc–implications from U-Pb and Sm-Nd analyses of the Oskarshamn-Jönköping Belt, southeastern Sweden. GFF 127, 149–157.
Marshall, L.J., Oliver, N.H.S., 2006. Monitoring fluid chemistry in iron oxide-copper-gold-related metasomatic processes, eastern Mt Isa Block, Australia. Geofluids 6, 45–66.
McKinney, S.T., Cottle, J.M., Lederer, G.W., 2015. Evaluating rare earth element (REE) mineralization mechanisms in Proterozoic gneiss, Music Valley, California. Geol. Soc. Am. Bull. 127, 1135–1152.
Monteiro, L.V.S., Xavier, R.P., Hitzman, M.W., Juliani, C., de Souza Filho, C.R., Carvalho, E.R., 2008. Mineral chemistry of ore and hydrothermal alteration at the Sossego iron oxide-copper-gold deposit, Carajás Mineral Province, Brazil. Ore Geol. Rev. 34, 317–336.
Morogan, V., 1989. Mass transfer and REE mobility during fenitization at Alnö, Sweden. Contrib. Mineral. Petr. 103, 25–34.
Morogan, V., Woolley, A., 1988. Fenitization at the Alnö carbonatite complex, Sweden: distribution, mineralogy and genesis. Contrib. Mineral. Petr. 100, 169–182.
Munoz, J.L., 1984. F-OH and Cl-OH exchange in micas with applications to hydrothermal ore deposits. Rev. Mineral. 13, 469–493.
Munoz, J.L., 1992. Calculation of HF and HCl fugacities from biotite compositions; revised equations. Geol. Soc. Am. Abstract Programs 24, 221.
Nadoll, P., Angerer, T., Mauk, J.L., French, D., Walshe, J., 2014. The chemistry of hydrothermal magnetite: a review. Ore Geol. Rev. 61, 1–32.
Nolte, N., Kleinhanns, I.C., Baero, W., Hansen, B.T., 2011. Petrography and whole-rock geochemical characteristics of Västervik granitoids to syenitoids, southeast Sweden: constraints on petrogenesis and tectonic setting at the southern margin of the Svecofennian domain. GFF 133, 173–194.
Nordenskjöld, I., 1910. Der Pegmatit von Ytterby. Bull. Geol. Inst. Uppsala 9, 183–228.
Ramberg, H., 1952. Chemical bonds and distribution of cations in silicates. J. Geol. 60, 331–355.
Reed, G.C., 2013. Amended and Restated Technical Report for Olserum REE Deposit, Southern Sweden. Tasman Metals, Vancouver, pp. 85.
Russel, R., 1969. Porphyroblastic differentiation in fleck gneiss from Västervik, Sweden. Geol. Fören. Stock. Förh. 91, 217–282.
Selby, D., Nesbitt, B.E., 2000. Chemical composition of biotite from the Casino porphyry Cu-Au-Mo mineralization, Yukon, Canada: evaluation of magmatic and hydrothermal fluid chemistry. Chem. Geol. 171, 77–93.
Seo, J.H., Guillong, M., Aerts, M., Zajacz, Z., Heinrich, C.A., 2011. Microanalysis of S, Cl, and Br in fluid inclusions by LA-ICP-MS. Chem. Geol. 284, 35–44.
Sjöqvist, A.S.L., Cornell, D.H., Andersen, T., Erambert, M., Ek, M., Leijd, M., 2013. Three compositional varieties of rare-earth element ore: eudialyte-group minerals from the Norra Kärr alkaline complex, southern Sweden. Minerals 3, 94–120.
Sjöqvist, A.S.L., Cornell, D.H., Andersen, T., Christensson, U.I., Berg, J.T., 2017. Magmatic age of rare-earth element and zirconium mineralisation at the Norra Kärr alkaline complex, southern Sweden, determined by U-Pb and Lu-Hf analyses of metasomatic zircon and eudialyte. Lithos 294–295, 73–86.
Slack, J.F., 1996. Tourmaline associations with hydrothermal ore deposits. Rev. Mineral. 33, 559–644.
Smeds, S.A., 1990. Regional trends in mineral assemblages of Swedish Proterozoic granitic pegmatites and their geological significance. Geol. Fören. Stock. Förh. 112, 517–534.
Streckeisen, A.L., LeMaitre, R.W., 1979. Chemical approximation to modal QAPF classification of the igneous rocks. Neues. Jb. Miner. 136, 169–206.
Sultan, L., Claesson, S., Plink-Björklund, P., 2005. Proterozoic and Archaean ages of detrital zircon from the Palaeoproterozoic Västervik Basin, SE Sweden: implications for provenance and timing of deposition. GFF 127, 17–24.
Sun, S., McDonough, W.F., 1989. Chemical and isotopic systematics of oceanic basalts: implications for mantle composition and processes. Geol. Soc. Lond. Spec. Pub. 42, 313–345.
Sundblad, K., 2003. Metallogeny of gold in the Precambrian of northern Europe. Econ. Geol. 98, 1271–1290.
Tegengren, F.R., 1924. Sveriges ädlare malmer och bergverk. Sveriges Geologiska Undersökning Ca 17, 406 pp.
Uytenbogaardt, W., 1960. Uranium mineralization in the Västervik area. Int. Geol.

Congress 15, 114–122.
Van Hinsberg, V.J., Henry, D.J., Dutrow, B.L., 2011. Tourmaline as a petrogenetic forensic mineral: a unique recorder of its geological past. Elements 7, 327–332.
Welin, E., 1966a. Uranium mineralizations and age relationships in the Precambrian bedrock of central and southeastern Sweden. Geol. Fören. Stock. Förh. 88, 34–67.
Welin, E., 1966b. Two occurrences of uranium in Sweden – the Los cobalt deposit and the iron ores of the Västervik area. Geol. Fören. Stock. Förh. 87, 492–508.
Westra, L., Elbers, F.J., Sijperda, W.S., 1969. Investigations in the Västervik area, Southeastern Sweden: 1. Structural geology and genesis of the "younger" granites. Geol. Mijnbouw. 48, 529–544.
Wikström, A., Andersson, U.B., 2004. The Småland-Värmland belt – geological features of the Småland-Värmland belt along the Svecofennian margin, part I: from the Loftahammar to the Tiveden-Askersund areas. Geol. S. Finl. 37, 22–38.
Zen, E., 1988. Phase relations of peraluminous granitic rocks and their petrogenetic implications. Annu. Rev. Earth Pl. Sc. 16, 21–51.
Zhang, W., Lentz, D.R., Thorne, K.G., McFarlane, C., 2016. Geochemical characteristics of biotite from felsic intrusive rocks around the Sisson Brook W-Mo-Cu deposit, west-central New Brunswick: an indicator of halogen and oxygen fugacity of magmatic systems. Ore Geol. Rev. 77, 82–96.
Zhu, C., Sverjensky, D.A., 1991. Partitioning of F-Cl–OH between minerals and hydrothermal fluids. Geochim. Cosmochim. Acta 55, 1837–1858.
Zhu, C., Sverjensky, D.A., 1992. F-Cl-OH partitioning between biotite and apatite. Geochim. Cosmochim. Acta 56, 3435–3467.